

Adversarial Schrödinger Bridge Matching

Nikita Gushchin*
Skoltech[†]
Moscow, Russia
n.gushchin
@skoltech.ru

Daniil Selikhanovych*
Skoltech[†]
Moscow, Russia
daniil.selikhanovych
@skoltech.ru

Sergei Kholkin*
Skoltech[†]
Moscow, Russia
s.kholkin
@skoltech.ru

Evgeny Burnaev
Skoltech[†], AIRI[‡]
Moscow, Russia
e.burnaev
@skoltech.ru

Alexander Korotin
Skoltech[†], AIRI[‡]
Moscow, Russia
a.korotin
@skoltech.ru

Abstract

The Schrödinger Bridge (SB) problem offers a powerful framework for combining optimal transport and diffusion models. A promising recent approach to solve the SB problem is the Iterative Markovian Fitting (IMF) procedure, which alternates between Markovian and reciprocal projections of continuous-time stochastic processes. However, the model built by the IMF procedure has a long inference time due to using many steps of numerical solvers for stochastic differential equations. To address this limitation, we propose a novel Discrete-time IMF (D-IMF) procedure in which learning of stochastic processes is replaced by learning just a few transition probabilities in discrete time. Its great advantage is that in practice it can be naturally implemented using the Denoising Diffusion GAN (DD-GAN), an already well-established adversarial generative modeling technique. We show that our D-IMF procedure can provide the same quality of unpaired domain translation as the IMF, using only several generation steps instead of hundreds.



Figure 1: Our D-IMF approach performs unpaired image-to-image translation in just a few steps, achieving results comparable to the hundred-step IMF [43]. Celeba [30], *male*→*female* (128×128).

*Equal contribution. The author's order is determined randomly.

[†]Skolkovo Institute of Science and Technology

[‡]Artificial Intelligence Research Institute

1 Introduction

Recent generative models based on the Flow Matching [24] and Rectified Flows [27] show great potential as a successor of classical denoising diffusion models such as DDPM [15]. Both these approaches consider the same problem of learning an Ordinary Differential Equation (ODE) that interpolates one given distribution to the other one, e.g., noise to data. Thanks to the close connection to the theory of Optimal Transport (OT) problem [48], Flow Matching and Rectified Flows approaches typically have faster inference compared to classical diffusion models [29, 36]. Also, it was shown that they can outperform diffusion models on the high-resolution text-to-image synthesis: they even lie in the foundation of the recent Stable Diffusion 3 model [8].

The extension of Flow Matching and Rectified Flow approaches to the SDE are Bridge Matching (Markovian projection) and **Iterative Markovian fitting** (IMF) procedures [33, 43, 32], respectively. They also have a close connection with the OT theory. Specifically, it is known [43, 32] that IMF converges to the solution of the dynamic formulation of entropic optimal transport (EOT), also known as the Schrödinger Bridge (SB). However, learning continuous-time SDEs in IMF is non-trivial and, unfortunately, leads to **long inference** due to the necessity to use many steps of numerical solvers.

Contributions. This paper addresses the above-mentioned limitation of the existing Iterative Markovian Fitting (IMF) framework by introducing a novel approach to learn the Schrödinger Bridge.

1. **Theory I.** We introduce a Discrete Iterative Markovian Fitting (**D-IMF**) procedure (§3.2, 3.3), which innovatively applies discrete Markovian projection to solve the Schrödinger Bridge problem without relying on Stochastic Differential Equations. This approach significantly simplifies the inference process, enabling it to be accomplished (theoretically) in just a few evaluation steps.
2. **Theory II.** We derive closed-form update formulas for the D-IMF procedure when dealing with high-dimensional Gaussian distributions. This advancement permits a detailed empirical analysis of our method’s convergence rate and enhances its theoretical foundation (§3.4, 4.1).
3. **Practice.** For general data distributions available by samples, we propose an algorithm (**ASBM**) to implement the discrete Markovian projection and our D-IMF procedure in practice (§4.2). Our algorithm is based on adversarial learning and Denoising Diffusion GAN [49]. Our learned SB model uses just 4 evaluation steps for inference (§3.5) instead of hundreds of the basic IMF [43].

Notations. In the paper, we simultaneously work with the continuous stochastic processes and discrete stochastic processes in the D -dimensional Euclidean space \mathbb{R}^D . We denote by $\mathcal{P}(C([0, 1]), \mathbb{R}^D)$ the set of continuous stochastic processes with time $t \in [0, 1]$, i.e., the set of distributions on continuous trajectories $f : [0, 1] \rightarrow \mathbb{R}^D$. We use dW_t to denote the differential of the standard Wiener process.

To establish a link between continuous and discrete stochastic processes, we fix $N \geq 1$ intermediate time moments $0 = t_0 < t_1 < \dots < t_N < t_{N+1} = 1$ together with $t_0 = 0$ and $t_{N+1} = 1$. We consider discrete stochastic processes with those time-moments as the elements of the set $\mathcal{P}(\mathbb{R}^{D \times (N+2)})$ of probability distributions on $\mathbb{R}^{D \times (N+2)}$. Among such discrete processes, we are specifically interested in subset $\mathcal{P}_{2,ac}(\mathbb{R}^{D \times (N+2)}) \subset \mathcal{P}(\mathbb{R}^{D \times (N+2)})$ of absolutely continuous distributions on $\mathbb{R}^{D \times (N+2)}$ which have a finite second moment and entropy. For any such $q \in \mathcal{P}_{2,ac}(\mathbb{R}^{D \times (N+2)})$, we write $q(x_0, x_{t_1}, \dots, x_{t_N}, x_1)$ to denote its density at a point $(x_0, x_{t_1}, \dots, x_{t_N}, x_1) \in \mathbb{R}^{D \times (N+2)}$. For continuous process T , we denote by $p^T \in \mathcal{P}(\mathbb{R}^{D \times (N+2)})$ the discrete process which is the finite-dimensional projection of T to time moments $0 = t_0 < t_1 < \dots < t_N < t_{N+1} = 1$. For convenience we also use the notation $x_{\text{in}} = (x_{t_1}, \dots, x_{t_N})$ to denote the vector of all intermediate-time variables. In what follows, KL is a short notation for the Kullback-Leibler divergence.

2 Background

We start with recalling the Bridge Matching and Iterative Proportional Fitting procedures developed for continuous-time stochastic processes (§2.1). Next, we discuss the Schrödinger Bridge problem, the solution to which is the unique fixed point of Iterative Markovian Fitting procedure (§2.2).

2.1 Bridge Matching and Iterative Markovian Fitting Procedures

Modern diffusion and flow generative modeling are mainly about the construction of a model that interpolates one probability distribution $p_0 \in \mathcal{P}_{2,ac}(\mathbb{R}^D)$ to some another probability distribution $p_1 \in \mathcal{P}_{2,ac}(\mathbb{R}^D)$. One of the general approaches for this task is the Bridge Matching [26, 28, 3].

Reciprocal processes. The Bridge Matching procedure is applied to the processes, which are represented as a mixture of Brownian Bridges. Consider the Wiener process W^ϵ with the volatility ϵ which start at p_0 , i.e., the process given by the SDE: $dx_t = \sqrt{\epsilon}dW_t, x_0 \sim p_0$. Let $W^\epsilon_{|x_0, x_1}$ denote

the stochastic process W^ϵ conditioned on values x_0, x_1 at times $t = 0, 1$, respectively. This process $W_{|x_0, x_1}^\epsilon$ is called the Brownian Bridge [16, Chapter 9]. For some $q(x_0, x_1) \in \mathcal{P}_{2,ac}(\mathbb{R}^{D \times 2})$ with $q(x_0) = p_0(x_0)$ and $q(x_1) = p_1(x_1)$ the process $T_q \stackrel{\text{def}}{=} \int W_{|x_0, x_1}^\epsilon dq(x_0, x_1)$ is called the mixture of Brownian Bridges. Following [43], we say that mixtures of Brownian Bridges form a *reciprocal class* of processes (for the Brownian Bridge). For brevity, we call these processes just reciprocal processes.

Bridge matching [26, 28]. The goal of Bridge Matching (with the Brownian Bridge) is to construct continuous-time Markovian process T from p_0 to p_1 in the form of SDE: $dx_t = v(x_t, t)dt + \sqrt{\epsilon}dW_t$. This is achieved by using the *Markovian projection* of a reciprocal process $T_q = \int W_{|x_0, x_1}^\epsilon dq(x_0, x_1)$, which aims to find the Markovian process M which is the most similar to T_q in the sense of KL:

$$\text{proj}_{\mathcal{M}}(T_q) \stackrel{\text{def}}{=} \arg \min_{M \in \mathcal{M}} \text{KL}(T_q \| M),$$

where $\mathcal{M} \subset \mathcal{P}(C([0, 1]), \mathbb{R}^D)$ is the set of all Markovian processes. For the Brownian Bridge $W_{|x_0, x_1}^\epsilon$ it is known [43, 11] that the SDE and the drift $v(x_t, t)$ of $\text{proj}_{\mathcal{M}}(T_q)$ is given by:

$$dx_t = v(x_t, t)dt + \sqrt{\epsilon}dW_t, \quad v(x_t, t) = \int \frac{x_1 - x_t}{1 - t} p^{T_q}(x_1 | x_t) dx_1,$$

where $p^{T_q}(x_1 | x_t)$ the conditional distribution of the stochastic process T_q at time moments t and 1. The process $\text{proj}_{\mathcal{M}}(T_q)$ has the same time marginal distributions $p^{T_q}(x_t)$ as the original Brownian bridge mixture T_q . However, the joint distribution $p^{T_q}(x_0, x_1)$ of T_q and the joint distribution $p^{\text{proj}_{\mathcal{M}}(T_q)}(x_0, x_1)$ of its markovian projection $\text{proj}_{\mathcal{M}}(T_q)$ do not coincide in the general case [6].

Iterative Markovian Fitting [43, 32, 1]. The Iterative Markovian Fitting procedure introduces a second type of projection of continuous-time stochastic processes called the *Reciprocal projection*. For a process T , the reciprocal projection $\text{proj}_{\mathcal{R}}(T)$ is defined by $\text{proj}_{\mathcal{R}}(T) = \int W_{|x_0, x_1}^\epsilon dp^T(x_0, x_1)$. The process $\text{proj}_{\mathcal{R}}(T)$ is called a projection, since:

$$\text{proj}_{\mathcal{R}}(T) = \arg \min_{R \in \mathcal{R}} \text{KL}(T \| R),$$

where $\mathcal{R} \subset \mathcal{P}(C([0, 1]), \mathbb{R}^D)$ is the set of all reciprocal processes. The Iterative Markovian Fitting procedure is an alternation between Markovian and Reciprocal projections:

$$T^{2l+1} = \text{proj}_{\mathcal{M}}(T^{2l}), \quad T^{2l+2} = \text{proj}_{\mathcal{R}}(T^{2l+1}),$$

It is known that the procedure converges to the unique stochastic process T^* , which is known as a solution to the Schrödinger Bridge (SB) problem between p_0 and p_1 . Furthermore, the SB T^* is the only process starting at p_0 and ending at p_1 that is both Markovian and reciprocal [22].

2.2 Schrödinger Bridge (SB) Problem

Schrödinger Bridge problem. The Schrödinger Bridge problem [40] was proposed in 1931/1932 by Erwin Schrödinger. For the Wiener prior W^ϵ Schrödinger Bridge problem between two probability distributions $p_0 \in \mathcal{P}_{2,ac}(\mathbb{R}^D)$ and $p_1 \in \mathcal{P}_{2,ac}(\mathbb{R}^D)$ is to minimize the following objective:

$$\min_{T \in \mathcal{F}(p_0, p_1)} \text{KL}(T \| W^\epsilon), \quad (1)$$

where $\mathcal{F}(p_0, p_1) \subset \mathcal{P}(C([0, 1]), \mathbb{R}^D)$ is the subset of stochastic processes which start at distribution p_0 (at the time $t = 0$) and end at p_1 (at $t = 1$). The Schrödinger Bridge has a unique solution, which is a diffusion process T^* described by the SDE: $dX_t = v^*(X_t, t)dt + \sqrt{\epsilon}dW_t$ [22]. The process T^* is called *the Schrödinger Bridge* and $v^* : \mathbb{R}^D \times [0, 1] \rightarrow \mathbb{R}^D$ is called *the optimal drift*.

From the practical point of view, the solution to the SB problem T^* tends to preserve the Euclidean distance between start point x_0 and endpoint x_1 . The equivalent form of SB problem, the static Schrödinger Bridge problem, explains this property more clearly.

Static Schrödinger Bridge problem. One may decompose $\text{KL}(T \| W^\epsilon)$ as [47, Appendix C]:

$$\text{KL}(T \| W^\epsilon) = \text{KL}(p^T(x_0, x_1) \| p^{W^\epsilon}(x_0, x_1)) + \int \text{KL}(T_{|x_0, x_1} \| W_{|x_0, x_1}^\epsilon) dp^T(x_0, x_1), \quad (2)$$

i.e., KL divergence between T and W^ϵ is a sum of two terms: the 1st represents the similarity of the processes' joint marginal distributions at start and finish times $t = 0, 1$, while the 2nd term represents

the average similarity of conditional processes $T_{|x_0, x_1}$ and $W_{|x_0, x_1}^\epsilon$. In [22, Proposition 2.3], the authors show that if T^* solves (1), then $T_{|x_0, x_1}^* = W_{|x_0, x_1}^\epsilon$. Hence, one may optimize (1) over T for which $T_{|x_0, x_1} = W_{|x_0, x_1}^\epsilon$ for every x_0, x_1 , i.e., over reciprocal processes T :

$$(1) = \min_{T \in \mathcal{F}(p_0, p_1) \cap \mathcal{R}} \text{KL}(p^T(x_0, x_1) || p^{W^\epsilon}(x_0, x_1)) = \min_{q \in \Pi(p_0, p_1)} \text{KL}(q(x_0, x_1) || p^{W^\epsilon}(x_0, x_1)), \quad (3)$$

where $\Pi(p_0, p_1) \subset \mathcal{P}_{2,ac}(\mathbb{R}^{D \times 2})$ is the set of joint probability distributions with marginal distributions p_0 and p_1 . Thus, the initial Schrödinger Bridge problem can be solved by optimizing only over a reciprocal process's joint distribution $q(x_0, x_1)$ at $t = 0, 1$. This problem is called the Static Schrödinger Bridge problem. In turn, the problem can be rewritten in the following way [12, Eq. 7]:

$$\min_{q \in \Pi(p_0, p_1)} \epsilon \text{KL}(q || p^{W^\epsilon}(x_0, x_1)) = \min_{q \in \Pi(p_0, p_1)} \int \frac{\|x_0 - x_1\|^2}{2} dq(x_0, x_1) - \epsilon \cdot \text{Entropy}(q) + C, \quad (4)$$

i.e., as finding a joint distribution $q(x_0, x_1)$ which tries to minimize the Euclidian distance $\frac{\|x-y\|^2}{2}$ between x_0 and x_1 (preserve similarity between x_0 and x_1), but with the addition of entropy regularizer $\epsilon \cdot \text{Entropy}(q)$ with the coefficient ϵ . Thus, the coefficient $\epsilon > 0$, which is the same for all problems considered above, regulates the stochastic or diversity of samples from $q(x_0, x_1)$. The last problem (4) is also known as the entropic optimal transport (EOT) problem [4, 35, 22].

3 Adversarial Schrödinger Bridge Matching (ASBM)

The IMF framework [32, 43] works with *continuous* time stochastic processes: it is built on the well-celebrated result that the only process which is both Markovian and reciprocal is the Schrödinger bridge T^* [22]. We derive an analogous theoretical result but for processes in *discrete* time. We provide proofs for all the theorems and propositions in Appendix B.

In §3.1, we give preliminaries on discrete processes with Markovian and reciprocal properties. In §3.2, we present the main theorem of our paper, which is the foundation of our **Discrete-time Iterative Markovian Fitting (D-IMF)** framework. In §3.3, we describe D-IMF procedure itself and prove that it allows us to solve the Schrödinger Bridge problem. In §3.4, we provide an analysis of applying our D-IMF for solving the Schrödinger Bridge between Gaussian distributions. In §3.5, we present the practical implementation of our D-IMF procedure using adversarial learning.

3.1 Discrete Markovian and reciprocal stochastic processes

Discrete reciprocal processes. We define the discrete reciprocal processes similarly to the continuous case by considering the finite-time projection of the Brownian bridge $W_{|x_0, x_1}^\epsilon$, which is given by:

$$p^{W^\epsilon}(x_{t_1}, \dots, x_{t_N} | x_0, x_1) = \prod_{n=1}^N p^{W^\epsilon}(x_{t_n} | x_{t_{n-1}}, x_1), \quad (5)$$

$$p^{W^\epsilon}(x_{t_n} | x_{t_{n-1}}, x_1) = \mathcal{N}(x_{t_n} | x_{t_{n-1}} + \frac{t_n - t_{n-1}}{1 - t_{n-1}}(x_1 - x_{t_{n-1}}), \epsilon \frac{(t_n - t_{n-1})(1 - t_n)}{1 - t_{n-1}}). \quad (6)$$

This joint distribution $p^{W^\epsilon}(x_{t_1}, \dots, x_{t_N} | x_0, x_1)$ defines a discrete stochastic process, which we call a discrete Brownian bridge. In turn, we say that a distribution $q \in \mathcal{P}_{2,ac}(\mathbb{R}^{D \times (N+2)})$ is a mixture of discrete Brownian bridges if it satisfies

$$q(x_0, x_{t_1}, \dots, x_{t_N}, x_1) = p^{W^\epsilon}(x_{t_1}, \dots, x_{t_N} | x_0, x_1) q(x_0, x_1),$$

where $q(x_0, x_1)$ denotes its joint marginal distribution of q at times 0, 1. That is, its "inner" part at times t_1, \dots, t_N is the discrete Brownian Bridge. We denote the set of all such mixtures as $\mathcal{R}(N) \subset \mathcal{P}_{2,ac}(\mathbb{R}^{D \times (N+2)})$ and call them discrete reciprocal processes.

Discrete Markovian processes. We say that a discrete process $q \in \mathcal{P}_{2,ac}(\mathbb{R}^{D \times (N+2)})$ is Markovian if its density can be represented in the following form (recall that $t_0 = 0, t_{N+1} = 1$):

$$q(x_0, x_{t_1}, x_{t_2}, \dots, x_{t_N}, x_1) = q(x_0) \prod_{n=1}^{N+1} q(x_{t_n} | x_{t_{n-1}}). \quad (7)$$

We denote the set of all such discrete Markovian processes as $\mathcal{M}(N) \subset \mathcal{P}_{2,ac}(\mathbb{R}^{D \times (N+2)})$.

3.2 Main Theorem

Theorem 3.1 (Discrete Markovian and reciprocal process is the solution of static SB). *Consider any discrete process $q \in \mathcal{P}_{2,ac}(\mathbb{R}^{D \times (N+2)})$, which is simultaneously reciprocal and markovian, i.e. $q \in \mathcal{R}(N)$ and $q \in \mathcal{M}(N)$ and has marginals $q(x_0) = p_0(x_0)$ and $q(x_1) = p_1(x_1)$:*

$$q(x_0, x_{t_1}, \dots, x_{t_N}, x_1) = p^{W^\epsilon}(x_{t_1}, \dots, x_{t_N} | x_0, x_1) q(x_0, x_1) = q(x_0) \prod_{n=1}^{N+1} q(x_{t_n} | x_{t_{n-1}}),$$

Then $q(x_0, x_{t_1}, \dots, x_{t_N}, x_1) = p^{T^}(x_0, x_{t_1}, \dots, x_{t_N}, x_1)$, i.e., it is the finite-dimensional projection of the Schrödinger Bridge T^* to the considered times. Moreover, its joint marginal $q(x_0, x_1)$ at times $t = 0, 1$ is the solution to the **static SB** problem (4) between p_0 and p_1 , i.e., $q(x_0, x_1) = p^{T^*}(x_0, x_1)$.*

Thus, to solve the static SB problem, it is enough to find a Markovian mixture of discrete Brownian bridges. To do so, we propose the Discrete-time Iterative Markovian Fitting (D-IMF) procedure.

3.3 Discrete-time Iterative Markovian Fitting (D-IMF) procedure

Similar to the IMF procedure, our proposed Discrete-time IMF is based on two alternating projections of discrete stochastic processes: reciprocal and Markovian. We start with the reciprocal projection.

Definition 3.2 (Discrete Reciprocal Projection). Assume that $q \in \mathcal{P}_{2,ac}(\mathbb{R}^{D \times (N+2)})$ is a discrete stochastic process. Then the reciprocal projection $\text{proj}_{\mathcal{R}}(q)$ is a discrete stochastic process with the joint distribution given by:

$$[\text{proj}_{\mathcal{R}}(q)](x_0, x_{t_1}, \dots, x_{t_N}, x_1) = p^{W^\epsilon}(x_{t_1}, \dots, x_{t_N} | x_0, x_1) q(x_0, x_1). \quad (8)$$

This projection takes the joint distribution of start and end points $q(x_0, x_1)$ and inserts the Brownian Bridge for intermediate time moments. The proposition below justifies the projection's name.

Proposition 3.3 (Discrete Reciprocal projection minimizes KL divergence with reciprocal processes). *Under mild assumptions, the reciprocal projection $\text{proj}_{\mathcal{R}}(q)$ of a stochastic discrete process $q \in \mathcal{P}_{2,ac}(\mathbb{R}^{D \times (N+2)})$ is the unique solution for the following optimization problem:*

$$\text{proj}_{\mathcal{R}}(q) = \arg \min_{r \in \mathcal{R}(N)} KL(q \| r). \quad (9)$$

Similarly to the discrete reciprocal projection, we introduce discrete Markovian projection.

Definition 3.4 (Discrete Markovian Projection). Assume that $q \in \mathcal{P}_{2,ac}(\mathbb{R}^{D \times (N+2)})$ is a discrete stochastic process. The Markovian projection of q is a discrete stochastic process $\text{proj}_{\mathcal{M}}(q) \in \mathcal{P}_{2,ac}(\mathbb{R}^{D \times (N+2)})$ whose joint distribution given by:

$$[\text{proj}_{\mathcal{M}}(q)](x_0, x_{t_1}, \dots, x_{t_N}, x_1) = q(x_0) \prod_{n=1}^{N+1} q(x_{t_n} | x_{t_{n-1}}). \quad (10)$$

As with the reciprocal projection, the following proposition justifies the name of the projection.

Proposition 3.5 (Discrete Markovian projection minimizes KL divergence with Markovian processes). *Under mild assumptions, the Markovian projection $\text{proj}_{\mathcal{M}}(q)$ of a stochastic discrete process $q \in \mathcal{P}_{2,ac}(\mathbb{R}^{D \times (N+2)})$ is a unique solution to the following optimization problem:*

$$\text{proj}_{\mathcal{M}}(q) = \arg \min_{m \in \mathcal{M}(N)} KL(q \| m). \quad (11)$$

Now we are ready to define our D-IMF procedure. For two given distributions $p_0 \in \mathcal{P}_{2,ac}(\mathbb{R}^D)$ and $p_1 \in \mathcal{P}_{2,ac}(\mathbb{R}^D)$ at times $t = 0$ and $t = 1$, respectively, it starts with any discrete Brownian mixture $p^{W^\epsilon}(x_{t_1}, \dots, x_{t_N} | x_0, x_1) q(x_0, x_1)$, where $q(x_0, x_1) \in \Pi(p_0, p_1) \cap \mathcal{P}_{2,ac}(\mathbb{R}^{D \times 2})$. Then, it constructs the following sequence of discrete stochastic processes:

$$q^{2l+1} = \text{proj}_{\mathcal{M}}(q^{2l}), \quad q^{2l+2} = \text{proj}_{\mathcal{R}}(q^{2l+1}). \quad (12)$$

Theorem 3.6 (D-IMF procedure converges to the the Schrödinger Bridge). *Under mild assumptions, the sequence q^l constructed by our D-IMF procedure converges in KL to p^{T^*} . In particular, $q^l(x_0, x_1)$ convergence to the solution $p^{T^*}(x_0, x_1)$ of the static SB. Namely, we have*

$$\lim_{l \rightarrow \infty} KL(q^l \| p^{T^*}) = 0, \quad \text{and} \quad \lim_{l \rightarrow \infty} KL(q^l(x_0, x_1) \| p^{T^*}(x_0, x_1)) = 0.$$

3.4 Closed form Updates of D-IMF for Gaussian Distributions

In this section, we show that our D-IMF updates (12) can be derived in the closed form for the Gaussian case. Let $p_0 = \mathcal{N}(x_0|\mu_0, \Sigma_0)$ and $p_1 = \mathcal{N}(x_1|\mu_1, \Sigma_1)$ be Gaussians. Consider any initial discrete Gaussian process $q \in \mathcal{P}_{2,ac}(\mathbb{R}^{D \times (N+2)})$ that has joint distribution $q(x_0, x_1) \in \Pi(p_0, p_1)$:

$$x_{01} \stackrel{\text{def}}{=} \begin{pmatrix} x_0 \\ x_1 \end{pmatrix}, \quad \mu_{01} \stackrel{\text{def}}{=} \begin{pmatrix} \mu_0 \\ \mu_1 \end{pmatrix}, \quad \Sigma = \begin{pmatrix} \Sigma_0 & \Sigma_{\text{cov}} \\ \Sigma_{\text{cov}}^T & \Sigma_1 \end{pmatrix}, \quad q(x_0, x_1) \stackrel{\text{def}}{=} \mathcal{N}(x_{01}|\mu_{01}, \Sigma) \quad (13)$$

where $\Sigma \in \mathbb{R}^{2D \times 2D}$ is positive definite and symmetric and Σ_{cov} is the covariance of x_0 and x_1 . In this case, the result of updates (12) is always a discrete Gaussian processes with specific parameters. To show this, we introduce two auxiliary matrices $U \in \mathbb{R}^{N \times 2}$ and $K \in \mathbb{R}^{ND \times ND}$:

$$U \stackrel{\text{def}}{=} \begin{pmatrix} (1-t_1)I_D & t_1 I_D \\ (1-t_2)I_D & t_2 I_D \\ \vdots & \vdots \\ (1-t_N)I_D & t_N I_D \end{pmatrix}, \quad K \stackrel{\text{def}}{=} \begin{pmatrix} t_1(1-t_1)I_D & t_1(1-t_2)I_D & \dots & t_1(1-t_N)I_D \\ t_1(1-t_2)I_D & t_2(1-t_2)I_D & \dots & t_2(1-t_N)I_D \\ \vdots & \vdots & \dots & \vdots \\ t_1(1-t_N)I_D & t_2(1-t_N)I_D & \dots & t_N(1-t_N)I_D \end{pmatrix}$$

Here I_D is an identity matrix with the shape $D \times D$. Below we present updates for both projections.

Theorem 3.7 (Reciprocal projection of a process whose joint marginal distribution is Gaussian). *Assume that $q \in \mathcal{P}_{2,ac}(\mathbb{R}^{D \times (N+2)})$ has Gaussian joint distribution $q(x_0, x_1)$ given by (13). Then*

$$[\text{proj}_{\mathcal{R}}q](x_{in}, x_0, x_1) = \mathcal{N}\left(\begin{pmatrix} x_{in} \\ x_{01} \end{pmatrix} \middle| \begin{pmatrix} U\mu_{01} \\ \mu_{01} \end{pmatrix}, \Sigma_R\right), \quad \Sigma_R \stackrel{\text{def}}{=} \begin{pmatrix} \epsilon K + U^T \Sigma U & U \Sigma \\ (U \Sigma)^T & \Sigma \end{pmatrix} \quad (14)$$

Theorem 3.8 (Markovian projection of a discrete Gaussian process). *Assume that $q \in \mathcal{P}_{2,ac}(\mathbb{R}^{D \times (N+2)})$ is a discrete Gaussian process with $q(x_0, x_1)$ given by (13) and the density*

$$q(x_{in}, x_0, x_1) = \mathcal{N}\left(\begin{pmatrix} x_{in} \\ x_{01} \end{pmatrix} \middle| \begin{pmatrix} \mu_{in} \\ \mu_{01} \end{pmatrix}, \tilde{\Sigma}_R\right), \quad \mu_{in} = (\mu_{t_1}, \dots, \mu_{t_N}),$$

where μ_{in} and $\tilde{\Sigma}_R$ are some parameters of q . Then its Markovian projection is given by:

$$[\text{proj}_{\mathcal{M}}q](x_{in}, x_0, x_1) = q(x_0) \prod_{n=1}^{N+1} q(x_{t_n} | x_{t_{n-1}}), \quad q(x_{t_n} | x_{t_{n-1}}) = \mathcal{N}(x_{t_n} | \hat{\mu}_{t_n}(x_{t_{n-1}}), \hat{\Sigma}_{t_n}),$$

$$\hat{\mu}_{t_n}(x_{t_{n-1}}) = \mu_{t_n} + (\tilde{\Sigma}_R)_{t_n, t_{n-1}} ((\tilde{\Sigma}_R)_{t_{n-1}, t_{n-1}})^{-1} (x_{t_{n-1}} - \mu_{t_{n-1}}),$$

$$\hat{\Sigma}_{t_n} = (\tilde{\Sigma}_R)_{t_n, t_n} - (\tilde{\Sigma}_R)_{t_n, t_{n-1}} ((\tilde{\Sigma}_R)_{t_{n-1}, t_{n-1}})^{-1} ((\tilde{\Sigma}_R)_{t_n, t_{n-1}})^T.$$

In turn, the joint distribution $[\text{proj}_{\mathcal{M}}q](x_0, x_1)$ is given by

$$[\text{proj}_{\mathcal{M}}q](x_0, x_1) = \mathcal{N}\left(\begin{pmatrix} x_0 \\ x_1 \end{pmatrix} \middle| \begin{pmatrix} \mu_0 \\ \mu_1 \end{pmatrix}, \begin{pmatrix} \Sigma_0 & \Sigma_{01} \\ (\Sigma_{01})^T & \Sigma_1 \end{pmatrix}\right), \quad \Sigma_{01} = \prod_{n=1}^{N+1} (\tilde{\Sigma}_R)_{t_{n+1}, t_n} ((\tilde{\Sigma}_R)_{t_n, t_n})^{-1} \Sigma_0.$$

Here $(\tilde{\Sigma}_R)_{t_i, t_j}$ is the submatrix of $\tilde{\Sigma}_R$ denoting the covariance of x_{t_i} and x_{t_j} , while Σ_0 and Σ_1 are covariance matrices of x_0 and x_1 respectively.

Thus, if we start D-IMF from some discrete process q^0 with marginals $q^0(x_0) = p_0(x_0)$, $q^0(x_1) = p_1(x_1)$ and Gaussian $q(x_0, x_1)$, then at each iteration of our D-IMF procedure q^l will be discrete Gaussian process with the same marginals and eventually will converge to q^* . In §4.1, we use our derived closed-form to perform an experimental analysis of D-IMF's convergence depending on the number of intermediate time moments N and the value of coefficient ϵ .

3.5 Practical Implementation of D-IMF: ASBM Algorithm

To implement our D-IMF procedure in practice, one should choose the process q^0 and implement both discrete Markovian and reciprocal projections. Note that one is usually not interested in the processes' density but only needs the ability to sample endpoints x_1 (or trajectories $x_0, x_{t_1}, \dots, x_{t_N}, x_1$) given a starting point $x_0 (= x_{t_0})$. Thus, to solve SB between $p_0(x_0)$ and $p_1(x_1)$ one should choose q^0 to have start and end marginals $q^0(x_0) = p_0(x_0)$ and $q^0(x_1) = p_1(x_1)$ accessible by samples.

Implementation of the discrete reciprocal projection. The reciprocal projection (8) of a given discrete process $q(x_0, x_{in}, x_1)$ is easy if one can sample from $q(x_0, x_1)$. To sample from $\text{proj}_{\mathcal{R}}(q)$ it is

enough to sample first a pair $(x_0, x_1) \sim q(x_0, x_1)$ and then sample intermediate points x_{t_1}, \dots, x_{t_N} from the Brownian bridge $p^{W^\epsilon}(x_{t_1}, \dots, x_{t_N} | x_0, x_1)$. This can be straightforwardly done using the formula (5) where the involved distributions (6) are simple Gaussians which are easy to sample from.

Implementation of the discrete Markovian projection via DD-GAN. To find the Markovian projection (10) of a reciprocal process $q \in \mathcal{R}(N)$, one just needs to estimate the transition probabilities between sequential time moments, i.e., the set $\{q(x_{t_n} | x_{t_{n-1}})\}_{n=1}^{N+1}$ and use the starting marginal $[\text{proj}_{\mathcal{M}} q](x_0) = q(x_0) = p_0(x_0)$. The natural way to find transition probabilities is to set to parametrize all these distributions as $\{q_\theta(x_{t_n} | x_{t_{n-1}})\}_{n=1}^{N+1}$ and solve

$$\min_{\theta} \sum_{n=1}^{N+1} \mathbb{E}_{q(x_{t_{n-1}})} D_{\text{adv}}(q(x_{t_n} | x_{t_{n-1}}) || q_\theta(x_{t_n} | x_{t_{n-1}})), \quad (15)$$

where D_{adv} is some distance or divergence between probability distributions. In this case, a minimum of such loss is achieved when $q_\theta(x_{t_n} | x_{t_{n-1}}) = q(x_{t_n} | x_{t_{n-1}})$ for each $n \in \{1, 2, \dots, N+1\}$.

We note that a related setting is considered in the Denoising Denoising GANs (DD-GAN), see [49, Eq. 4]. The difference is in the nature of q : there q comes from the standard noising diffusion process, while in our case it is a given reciprocal process. Overall, the authors show that problems like (15) can be efficiently approached via time-conditioned GANs. Therefore, we naturally pick *DD-GAN approach as the backbone* to learn our discrete Markovian projection and use their best practices.

In short, following DD-GAN, we parameterize $q_\theta(x_{t_n} | x_{t_{n-1}})$ via a time-conditioned generator network $G_\theta(x_{t_{n-1}}, z, t_{n-1})$. As in DD-GAN, we use the non-saturating GAN loss [10] as D_{adv} , which optimizes softened reverse KL-divergence [42]. To optimize this loss, an additional conditional discriminator network $D(x_{t_{n-1}}, x_{t_n}, t_{n-1})$ is needed. We do not recall technical details here as they are the same as in DD-GAN. For further [details](#) on DD-GAN learning, we refer to Appendix D.1.

Note that after learning $\{q_\theta(x_{t_n} | x_{t_{n-1}})\}_{n=1}^{N+1}$ the sampling assumes to take sample from $q_0(x_0) = p(x_0)$ and then sample from $\{q_\theta(x_{t_n} | x_{t_{n-1}})\}_{n=1}^{N+1}$. Hence it is guaranteed that $q_0(x_0) = p(x_0)$, but there may be an approximation error in estimating $q_1(x_1) \approx p(x_1)$. This is due to the asymmetry of the definition of Markovian projection, i.e., it can be written in two equivalent ways:

$$[\text{proj}_{\mathcal{M}}(q)](x_0, x_{t_1}, \dots, x_{t_N}, x_1) = q(x_0) \prod_{n=1}^{N+1} q(x_{t_n} | x_{t_{n-1}}) = q(x_1) \prod_{n=1}^{N+1} q(x_{t_{n-1}} | x_{t_n}).$$

Analogously to the implementation of IMF [43, Algorithm 1], we address this asymmetry in our D-IMF by alternatively learning Markovian projection in forward and reverse directions. To learn Markovian projection in the reverse direction, we just need to use starting marginal $[\text{proj}_{\mathcal{M}} q](x_1) = p_1(x_1)$, parametrize $\{q_\eta(x_{t_{n-1}} | x_{t_n})\}_{n=1}^{N+1}$ and solve:

$$\min_{\eta} \sum_{n=1}^{N+1} \mathbb{E}_{q(x_{t_n})} D_{\text{adv}}(q(x_{t_{n-1}} | x_{t_n}) || q_\eta(x_{t_{n-1}} | x_{t_n})). \quad (16)$$

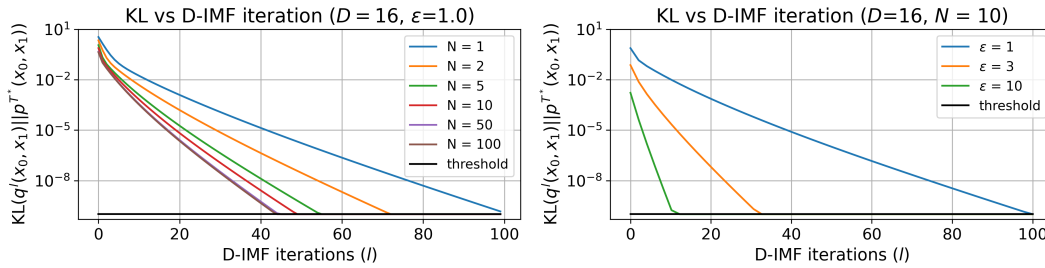
In this case $q(x_1) = p_1(x_1)$ is guaranteed, while $q(x_0) \approx p_0(x_0)$.

Implementation of the D-IMF procedure (ASBM algorithm). We start with initialization of q^0 by the reciprocal process. Depending on the setup we use initialization with the independent coupling, i.e. $q^0(x_0, x_1) = p_0(x_0)p_1(x_1)$ or a minibatch OT coupling [9, 36], see Appendix D.3 for details.

We follow the best practices of IMF [43] and in the Markovian projection steps, we alternately learn models in the direction $p_0 \rightarrow p_1$ and in the reverse direction $p_1 \rightarrow p_0$ by using functionals (15) and (16) respectively to avoid the accumulation of errors due to the asymmetry in the definition of the Markovian projection. For details, see Appendix D.2. At the reciprocal projection steps, we use the model $q_\theta(x_0, x_{\text{in}}, x_1)$ or $q_\eta(x_0, x_{\text{in}}, x_1)$ learned to approximate q^{2l+1} to sample pair (x_0, x_1) and then sample intermediate points from Brownian bridge. We use the term **outer iteration** (K) for a sequence of two reciprocal projections and two Markovian projections in different directions.

3.6 Relation to Prior Works

There exists a variety of algorithms for learning SB based on different underlying principles: dual form entropic optimal transport algorithms [5, 31, 21, 11, 12, 41], iterative proportional fitting (IPF) algorithms [47, 7, 2], bridge matching [45, 26] and iterative Markovian fitting (IMF) algorithms



(a) Dependence on the number of time steps N . (b) Dependence on the variance ϵ of the prior process.

Figure 2: Dependence of convergence of **our** D-IMF procedure on N and ϵ .

[43, 32, 25], adversarial algorithms [18], etc. We refer to [13] for a benchmark and to [21, Table 1] for a quick survey of many of them. In turn, in our paper, we specifically focus on the advancement of IMF-type algorithms [43, 32] as they are not only theoretically well-grounded but also closely connected to the rectified flow approach [27] which works well in large-scale generative modeling [29, 50]. Below we discuss the relation of our contributions (§1) to the prior works in IMF [43, 32].

Theory I. As we detailed in §2, basic IMF operates with stochastic processes in continuous time and iteratively performs Markovian and reciprocal projections. Our D-IMF procedure (§3) does the same but in the discrete time, so it might *deceptively* seem like our D-IMF is just an approximation of IMF. However, this is a misleading viewpoint. Indeed, the Markovian projection in the discrete time, in general, does not match with the continuous time Markovian projection. Still our D-IMF procedure *provably* converges to SB. Furthermore, D-IMF procedure can theoretically work with just one intermediate time step (when $N = 1$). Overall, its convergence rate varies depending on the number of intermediate points, see §4.1. Naturally, we conjecture that in the limit $N \rightarrow \infty$ (when the time steps t_1, \dots, t_N densely fill $[0, 1]$) our D-IMF behaves the same as IMF since the discrete and continuous Markovian projections start to be close, see discussion in [43, Appendix E].

Theory II. In §3.4, we derive the closed-form expression for our D-IMF updates in the Gaussian case. For the continuous IMF, there exists an analogous result [32, §6.1]. However, unlike our result, that one is not explicit in the sense that it requires solving the matrix-valued ODE [32, Eq. 39] to get the actual projection. The analytical solution is known only when $D = 1$, i.e., 1-dimensional case, see also [43, Appendix D]. In contrast, our Gaussian D-IMF updates work in any dimension D .

Practice. Default continuous-time IMF [43, 32] in practice is naturally implemented via the Bridge Matching approach which learns an SDE. In our case, at each D-IMF step we learn several transitional probabilities and do this via also well-established adversarial techniques. In this sense, our practical implementation differs – each approach is based on its own backbone – bridge matching vs. adversarial learning – and naturally inherits the benefits/drawbacks of the respective backbone. They are fairly well stated in the discussion of the generative learning trilemma in [49].

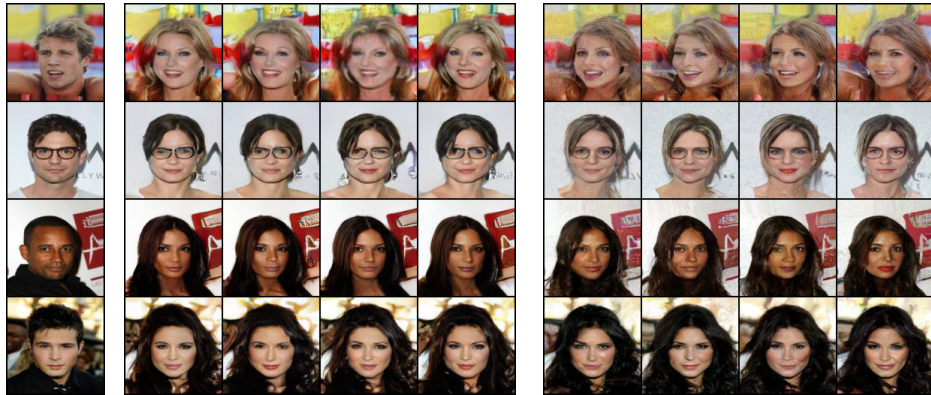
4 Experiments

We evaluate our adversarial SB matching (**ASBM**) algorithm, which implements our D-IMF procedure on setups with Gaussian distributions (§4.1) for which we have closed form update formulas (§3.4) and real image data distributions (§4.2). We additionally provide results for an illustrative 2D example in Appendix C.1, results for the Colored MNIST dataset in Appendix C.3, and results on the standard SB benchmark in Appendix C.2. The code for our algorithm and all experiments with it is written in PyTorch, is available in the supplementary materials, and will be made public. We provide all the technical details in Appendix D.

4.1 Gaussian-to-Gaussian Schrödinger Bridge

We analyze the convergence of our D-IMF procedure depending on the number of intermediate time steps $N \geq 1$ (we use $t_n = n/N + 1$) and the value $\epsilon > 0$ in the Gaussian case. In this case, the static SB solution $p^{T^*}(x_0, x_1)$ is analytically known, see, e.g., [17]. This provides us an opportunity to analyse how fast $\text{KL}(q^l(x_0, x_1) \| p^{T^*}(x_0, x_1))$ decreases when $l \rightarrow \infty$.

We conduct experiments by using our analytical formulas for D-IMF from §3.4. We follow setup from [12] and consider Schrödinger Bridge problem with the dimensionality $D = 16$ and $\epsilon \in \{1, 3, 10\}$ for centered Gaussians $p_0 = \mathcal{N}(0, \Sigma_0)$ and $p_1 = \mathcal{N}(0, \Sigma_1)$. To construct Σ_0 and Σ_1 , sample their eigenvectors from the uniform distribution on the unit sphere and sample their eigenvalues from the log uniform distribution on $[-\log 2, \log 2]$. We use the same p_0 and p_1 for all experiments.



(a) $x \sim p_0$ (b) ASBM (ours), $\epsilon = 1$ (lower diversity) FID = 16.08, NFE = 4. (c) DSBM [43], $\epsilon = 1$ (lower diversity) FID = 37.8, NFE = 100.



(d) $x \sim p_0$ (e) ASBM (ours), $\epsilon = 10$ (higher diversity) FID = 17.44, NFE = 4. (f) DSBM [43], $\epsilon = 10$ (higher diversity) FID = 89.19, NFE = 100.

Figure 3: Results of Celeba, *male* \rightarrow *female* translation learned with ASBM (ours), and DSBM learned on Celeba dataset with 128 resolution size for $\epsilon \in \{1, 10\}$.

We start our D-IMF procedure from the reciprocal process with $q^0(x_0, x_1) = p_0(x_0)p_1(x_1)$, i.e. from the independent joint distribution at times $t = 0, 1$. We present the convergence plots in Figures 2a and 2b. In both plots, we use 10^{-10} as a threshold corresponding to the exact matching of distributions to prevent numerical instabilities. We see that in all the cases, our D-IMF procedure shows an **exponential rate of convergence**. As we can see from Figure 2a, the convergence speed dependence on N quickly saturates. Thus, even several time moments, e.g., $N = 5$, provide quick convergence speed. From Figure 2b, we clearly see that the convergence speed is highly influenced by the chosen value of the parameter ϵ . For instance, the transition from $\epsilon = 1$ to $\epsilon = 10$ requires ten times more D-IMF iterations. Thus, this hyperparameter may be important in practical problems.

4.2 Unpaired Image-to-image Translation

To test our approach on real data, we consider the unpaired image-to-image translation setup of learning *male* \rightarrow *female* faces of Celeba dataset [30]. We use 10% of *male* and *female* images as the test set for evaluation. We train our ASBM algorithm based on the D-IMF procedure with $\epsilon = 1$ and $\epsilon = 10$. Following the best practices of DD-GAN [49], we use $N = 3$, intermediate times $t_1 = \frac{1}{4}, t_2 = \frac{2}{4}, t_3 = \frac{3}{4}$ and $K = 5$ outer iterations of D-IMF. We provide qualitative results and the FID metric [14] on the test set in Figures 3b and 3e. Since we use $N = 3$ intermediate time moments, our algorithm requires only 4 number of function evaluations (NFE) at the inference stage.

We focus our comparison on the DSBM algorithm based on the IMF-procedure [43] since it is closely related to our method. We train DSBM following the authors [43] and use NFE = 100. As well as for ASBM, we use 5 outer iterations of IMF, corresponding to the same number of reciprocal and Markovian projections, but for continuous processes. We use approximately the same number of parameters of neural networks used for models in Markovian projections for ASBM and DSBM (see Appendix D.3). For other details, see Appendix D.4. We present results for DSBM in Figure 3c and Figure 3f. Our algorithm provides better results while using only 4 evaluation steps. Further additional results for ASBM and DSBM algorithms on the Celeba dataset are presented in Appendix E.

Thus, our D-IMF procedure allows us to solve the Schrödinger Bridge efficiently without learning the time-continuous stochastic process, which in turn speeds up inference by an order of magnitude. This aligns with the results obtained in the Gaussian-to-Gaussian setups about exponentially fast convergence of D-IMF even with several intermediate time moments.

5 Discussion

Potential impact. Beside the pure speed up of the inference of IMF, we want to point to another great advantage of our developed D-IMF framework. In the continuous IMF, one is forced to do Markovian projection via time-consuming learning of continuous-time SDEs (using procedures like bridge matching). In our D-IMF framework, one needs to **learn several transition probabilities**. We do this via adversarial learning [10], but actually this can be done **using almost any other generative modeling technique** (moment matching [23], normalizing flows [20, 37], energy-based models [51], score-based models [44], etc.). We believe that this observation opens great possibilities for ML community to further explore and improve generative modeling algorithms based on Schrödinger Bridges, Markovian projections (bridge matching) and related techniques, e.g., flow matching [24].

Limitations and broader impact are discussed in Appendix A.

References

- [1] Rob Brekelmans and Kirill Neklyudov. On schrödinger bridge matching and expectation maximization. In *NeurIPS 2023 Workshop Optimal Transport and Machine Learning*, 2023.
- [2] Tianrong Chen, Guan-Hong Liu, and Evangelos Theodorou. Likelihood training of schrödinger bridge using forward-backward sdes theory. In *International Conference on Learning Representations*, 2021.
- [3] Hyungjin Chung, Jeongsol Kim, and Jong Chul Ye. Direct diffusion bridge using data consistency for inverse problems. *Advances in Neural Information Processing Systems*, 36, 2024.
- [4] Marco Cuturi. Sinkhorn distances: Lightspeed computation of optimal transport. *Advances in neural information processing systems*, 26, 2013.
- [5] Max Daniels, Tyler Maunu, and Paul Hand. Score-based generative neural networks for large-scale optimal transport. *Advances in neural information processing systems*, 34:12955–12965, 2021.
- [6] Valentin De Bortoli, Guan-Hong Liu, Tianrong Chen, Evangelos A Theodorou, and Weillie Nie. Augmented bridge matching. *arXiv preprint arXiv:2311.06978*, 2023.
- [7] Valentin De Bortoli, James Thornton, Jeremy Heng, and Arnaud Doucet. Diffusion schrödinger bridge with applications to score-based generative modeling. *Advances in Neural Information Processing Systems*, 34:17695–17709, 2021.
- [8] Patrick Esser, Sumith Kulal, Andreas Blattmann, Rahim Entezari, Jonas Müller, Harry Saini, Yam Levi, Dominik Lorenz, Axel Sauer, Frederic Boesel, et al. Scaling rectified flow transformers for high-resolution image synthesis. *arXiv preprint arXiv:2403.03206*, 2024.
- [9] Kilian Fatras, Younes Zine, Rémi Flamary, Remi Gribonval, and Nicolas Courty. Learning with minibatch wasserstein: asymptotic and gradient properties. In *International Conference on Artificial Intelligence and Statistics*, pages 2131–2141. PMLR, 2020.
- [10] Ian Goodfellow, Jean Pouget-Abadie, Mehdi Mirza, Bing Xu, David Warde-Farley, Sherjil Ozair, Aaron Courville, and Yoshua Bengio. Generative adversarial nets. In *Advances in neural information processing systems*, pages 2672–2680, 2014.
- [11] Nikita Gushchin, Sergei Kholkin, Evgeny Burnaev, and Alexander Korotin. Light and optimal schrödinger bridge matching. *arXiv preprint arXiv:2402.03207*, 2024.
- [12] Nikita Gushchin, Alexander Kolesov, Alexander Korotin, Dmitry Vetrov, and Evgeny Burnaev. Entropic neural optimal transport via diffusion processes. In *Advances in Neural Information Processing Systems*, 2023.
- [13] Nikita Gushchin, Alexander Kolesov, Petr Mokrov, Polina Karpikova, Andrey Spiridonov, Evgeny Burnaev, and Alexander Korotin. Building the bridge of schrödinger: A continuous entropic optimal transport benchmark. In *Thirty-seventh Conference on Neural Information Processing Systems Datasets and Benchmarks Track*, 2023.

- [14] Martin Heusel, Hubert Ramsauer, Thomas Unterthiner, Bernhard Nessler, and Sepp Hochreiter. GANs trained by a two time-scale update rule converge to a local nash equilibrium. In *Advances in neural information processing systems*, pages 6626–6637, 2017.
- [15] Jonathan Ho, Ajay Jain, and Pieter Abbeel. Denoising diffusion probabilistic models. *Advances in neural information processing systems*, 33:6840–6851, 2020.
- [16] Oliver Ibe. *Markov processes for stochastic modeling*. Newnes, 2013.
- [17] Hicham Janati, Boris Muzellec, Gabriel Peyré, and Marco Cuturi. Entropic optimal transport between unbalanced gaussian measures has a closed form. *Advances in neural information processing systems*, 33:10468–10479, 2020.
- [18] Beomsu Kim, Gihyun Kwon, Kwanyoung Kim, and Jong Chul Ye. Unpaired image-to-image translation via neural schrödinger bridge. In *The Twelfth International Conference on Learning Representations*, 2024.
- [19] Diederik P Kingma and Jimmy Ba. Adam: A method for stochastic optimization. *arXiv preprint arXiv:1412.6980*, 2014.
- [20] Durk P Kingma and Prafulla Dhariwal. Glow: Generative flow with invertible 1x1 convolutions. *Advances in neural information processing systems*, 31, 2018.
- [21] Alexander Korotin, Nikita Gushchin, and Evgeny Burnaev. Light schrödinger bridge. In *International Conference on Learning Representations*, 2024.
- [22] Christian Léonard. A survey of the schrödinger problem and some of its connections with optimal transport. *arXiv preprint arXiv:1308.0215*, 2013.
- [23] Yujia Li, Kevin Swersky, and Rich Zemel. Generative moment matching networks. In *International conference on machine learning*, pages 1718–1727. PMLR, 2015.
- [24] Yaron Lipman, Ricky TQ Chen, Heli Ben-Hamu, Maximilian Nickel, and Matthew Le. Flow matching for generative modeling. In *The Eleventh International Conference on Learning Representations*, 2022.
- [25] Guan-Horng Liu, Yaron Lipman, Maximilian Nickel, Brian Karrer, Evangelos Theodorou, and Ricky TQ Chen. Generalized schrödinger bridge matching. In *The Twelfth International Conference on Learning Representations*, 2023.
- [26] Guan-Horng Liu, Arash Vahdat, De-An Huang, Evangelos A Theodorou, Weili Nie, and Anima Anandkumar. Image-to-image schrödinger bridge. In *Proceedings of the 40th International Conference on Machine Learning*, pages 22042–22062, 2023.
- [27] Xingchao Liu, Chengyue Gong, et al. Flow straight and fast: Learning to generate and transfer data with rectified flow. In *The Eleventh International Conference on Learning Representations*, 2022.
- [28] Xingchao Liu, Lemeng Wu, Mao Ye, et al. Let us build bridges: Understanding and extending diffusion generative models. In *NeurIPS 2022 Workshop on Score-Based Methods*, 2022.
- [29] Xingchao Liu, Xiwen Zhang, Jianzhu Ma, Jian Peng, et al. InstafLOW: One step is enough for high-quality diffusion-based text-to-image generation. In *The Twelfth International Conference on Learning Representations*, 2023.
- [30] Ziwei Liu, Ping Luo, Xiaogang Wang, and Xiaoou Tang. Deep learning face attributes in the wild. In *Proceedings of International Conference on Computer Vision (ICCV)*, December 2015.
- [31] Petr Mokrov, Alexander Korotin, Alexander Kolesov, Nikita Gushchin, and Evgeny Burnaev. Energy-guided entropic neural optimal transport. In *The Twelfth International Conference on Learning Representations*, 2024.
- [32] Stefano Peluchetti. Diffusion bridge mixture transports, schrödinger bridge problems and generative modeling. *Journal of Machine Learning Research*, 24(374):1–51, 2023.
- [33] Stefano Peluchetti. Non-denoising forward-time diffusions. *arXiv preprint arXiv:2312.14589*, 2023.
- [34] Kaare Brandt Petersen, Michael Syskind Pedersen, et al. The matrix cookbook. *Technical University of Denmark*, 7(15):510, 2008.
- [35] Gabriel Peyré, Marco Cuturi, et al. Computational optimal transport. *Foundations and Trends® in Machine Learning*, 11(5-6):355–607, 2019.

- [36] Aram-Alexandre Pooladian, Heli Ben-Hamu, Carles Domingo-Enrich, Brandon Amos, Yaron Lipman, and Ricky TQ Chen. Multisample flow matching: Straightening flows with minibatch couplings. In *International Conference on Machine Learning*, pages 28100–28127. PMLR, 2023.
- [37] Danilo Rezende and Shakir Mohamed. Variational inference with normalizing flows. In *International conference on machine learning*, pages 1530–1538. PMLR, 2015.
- [38] Olaf Ronneberger, Philipp Fischer, and Thomas Brox. U-net: Convolutional networks for biomedical image segmentation. In *Medical image computing and computer-assisted intervention–MICCAI 2015: 18th international conference, Munich, Germany, October 5-9, 2015, proceedings, part III 18*, pages 234–241. Springer, 2015.
- [39] Ludger Ruschendorf. Convergence of the iterative proportional fitting procedure. *The Annals of Statistics*, pages 1160–1174, 1995.
- [40] Erwin Schrödinger. *Über die umkehrung der naturgesetze*. Verlag der Akademie der Wissenschaften in Kommission bei Walter De Gruyter u . . . , 1931.
- [41] Vivien Seguy, Bharath Bhushan Damodaran, Remi Flamary, Nicolas Courty, Antoine Rolet, and Mathieu Blondel. Large scale optimal transport and mapping estimation. In *International Conference on Learning Representations*, 2018.
- [42] Matt Shannon, Ben Poole, Soroosh Mariooryad, Tom Bagby, Eric Battenberg, David Kao, Daisy Stanton, and RJ Skerry-Ryan. Non-saturating gan training as divergence minimization. *arXiv preprint arXiv:2010.08029*, 2020.
- [43] Yuyang Shi, Valentin De Bortoli, Andrew Campbell, and Arnaud Doucet. Diffusion schrödinger bridge matching. In *Thirty-seventh Conference on Neural Information Processing Systems*, 2023.
- [44] Yang Song and Stefano Ermon. Generative modeling by estimating gradients of the data distribution. *Advances in neural information processing systems*, 32, 2019.
- [45] Alexander Tong, Nikolay Malkin, Kilian Fatras, Lazar Atanackovic, Yanlei Zhang, Guillaume Hugué, Guy Wolf, and Yoshua Bengio. Simulation-free schrödinger bridges via score and flow matching. *arXiv preprint arXiv:2307.03672*, 2023.
- [46] Tim Van Erven and Peter Harremoës. Rényi divergence and kullback-leibler divergence. *IEEE Transactions on Information Theory*, 60(7):3797–3820, 2014.
- [47] Francisco Vargas, Pierre Thodoroff, Austen Lamacraft, and Neil Lawrence. Solving schrödinger bridges via maximum likelihood. *Entropy*, 23(9):1134, 2021.
- [48] Cédric Villani. *Optimal transport: old and new*, volume 338. Springer Science & Business Media, 2008.
- [49] Zhisheng Xiao, Karsten Kreis, and Arash Vahdat. Tackling the generative learning trilemma with denoising diffusion gans. In *International Conference on Learning Representations*, 2021.
- [50] Hanshu Yan, Xingchao Liu, Jiachun Pan, Jun Hao Liew, Qiang Liu, and Jiashi Feng. Perflow: Piecewise rectified flow as universal plug-and-play accelerator, 2024.
- [51] Yang Zhao, Jianwen Xie, and Ping Li. Learning energy-based generative models via coarse-to-fine expanding and sampling. In *International Conference on Learning Representations*, 2020.

A Limitations and Future Work

Adversarial training. It is a generic knowledge that the adversarial training may be non trivial to conduct due to instabilities, mode collapse and related issues. While we mention this aspect, we do not treat it to be a serious limitation. Indeed, our ASBM algorithm relies on the already well-established and carefully tuned DD-GAN [49] technique as a backbone. The latter is specifically designed to address many such limitations and is known to score good metrics in generative modeling.

Theoretical convergence rate. We derive the generic convergence result for our D-IMF procedure (Theorem 3.6) but without the particular convergence rate. Empirically we observe the exponentially fast convergence (§4.1), but theoretically proving this rate is an important task for the future work.

Broader Impact. This paper presents work whose goal is to advance the field of Artificial Intelligence, Machine Learning and Generative Modeling. There are many potential societal consequences of our work, none which we feel must be specifically highlighted here.

B Proofs

Here we provide the proof of our theoretical results one-by-one. Additionally, we introduce and prove several auxiliary results to simplify the derivation of the main results.

B.1 Proofs for Statements in Section 3.2

In our view, the proof of our main Theorem here is the most interesting and insightful (among all the proofs in the paper) as it uses some tricky mathematics, especially in its stage 2. In turn, stage 1 of the proof is inspired by the recent insights of [13, Theorem 3.2] about the characterization of static Schrödinger Bridge solutions [22] and manipulations with KL for SB in [21, 11].

Proof of Theorem 3.1. We split the proof in 2 stages. The 1st is auxiliary for the 2nd.

Stage 1. Here we show that if some $q(x_0, x_1) \in \mathcal{P}_{2,ac}(\mathbb{R}^{D \times 2})$ with marginals $p_0(x_0) = q(x_0)$ and $p_1(x_1) = q(x_1)$ has the density in the form

$$q(x_0, x_1) = q(x_0) \widehat{C}(x_0) \exp\left(-\frac{\|x_1 - x_0\|^2}{2\epsilon}\right) \widehat{\phi}(x_1),$$

then it solves the Static SB between distributions $p_0(x_0)$ and $p_1(x_1)$. It is known [22], that the solution $q^*(x_0, x_1) \stackrel{\text{def}}{=} p^{T^*}(x_0, x_1)$ of Static SB between p_0 and p_1 has the density:

$$q^*(x_0, x_1) = \psi^*(x_0) \exp\left(-\frac{\|x_1 - x_0\|^2}{2\epsilon}\right) \phi^*(x_1).$$

Hence, the conditional density $q^*(x_1|x_0)$ is expressed as:

$$q^*(x_1|x_0) = \underbrace{\frac{\psi^*(x_0)}{p_0(x_0)}}_{\stackrel{\text{def}}{=} C^*(x_0)} \exp\left(-\frac{\|x_1 - x_0\|^2}{2\epsilon}\right) \phi^*(x_1) = C^*(x_0) \exp\left(-\frac{\|x_1 - x_0\|^2}{2\epsilon}\right) \phi^*(x_1).$$

Thus, both $q(x_0, x_1)$ and $q^*(x_0, x_1)$ have their densities in the same functional form and the same marginals $q(x_0) = q^*(x_0) = p_0(x_0)$ and $q(x_1) = q^*(x_1) = p_1(x_1)$. However, we want to prove that in this case $q(x_0, x_1)$ and $q^*(x_0, x_1)$ are equal, i.e., $\text{KL}(q^*||q) = 0$.

$$\begin{aligned} \text{KL}(q^*(x_0, x_1)||q(x_0, x_1)) &= \int \log \frac{q^*(x_0, x_1)}{q(x_0, x_1)} q^*(x_0, x_1) dx_0 dx_1 = \\ &= \int \log \frac{p_0(x_0) q^*(x_1|x_0)}{p_0(x_0) q(x_1|x_0)} q^*(x_0, x_1) dx_0 dx_1 = \\ &= \int \log \frac{C^*(x_0) \exp\left(-\frac{\|x_1 - x_0\|^2}{2\epsilon}\right) \phi^*(x_1)}{\widehat{C}(x_0) \exp\left(-\frac{\|x_1 - x_0\|^2}{2\epsilon}\right) \widehat{\phi}(x_1)} q^*(x_0, x_1) dx_0 dx_1 = \end{aligned}$$

$$\begin{aligned}
& \int (\log \frac{C^*(x_0)}{\widehat{C}(x_0)} + \log \frac{\phi^*(x_1)}{\widehat{\phi}(x_1)}) q^*(x_0, x_1) dx_0 dx_1 = \\
& \int \log \frac{C^*(x_0)}{\widehat{C}(x_0)} q^*(x_0, x_1) dx_0 dx_1 + \int \log \frac{\phi^*(x_1)}{\widehat{\phi}(x_1)} q^*(x_0, x_1) dx_0 dx_1 = \\
& \int \log \frac{C^*(x_0)}{\widehat{C}(x_0)} p_0(x_0) dx_0 + \int \log \frac{\phi^*(x_1)}{\widehat{\phi}(x_1)} p_1(x_1) dx_1 = \\
& \int \log \frac{C^*(x_0)}{\widehat{C}(x_0)} q(x_0, x_1) dx_0 dx_1 + \int \log \frac{\phi^*(x_1)}{\widehat{\phi}(x_1)} q(x_0, x_1) dx_0 dx_1 = \\
& \int (\log \frac{C^*(x_0)}{\widehat{C}(x_0)} + \log \frac{\phi^*(x_1)}{\widehat{\phi}(x_1)}) q(x_0, x_1) dx_0 dx_1 = \\
& \int \log \frac{C^*(x_0) \phi^*(x_1)}{\widehat{C}(x_0) \widehat{\phi}(x_1)} q(x_0, x_1) dx_0 dx_1 = \\
& \int \log \frac{C^*(x_0) \exp(-\frac{\|x_1 - x_0\|^2}{2\epsilon}) \phi^*(x_1)}{\widehat{C}(x_0) \exp(-\frac{\|x_1 - x_0\|^2}{2\epsilon}) \widehat{\phi}(x_1)} q(x_0, x_1) dx_0 dx_1 = \\
& \int \log \frac{q^*(x_1|x_0)}{q(x_1|x_0)} q(x_0, x_1) dx_0 dx_1 = \\
& \int \log \frac{p_0(x_0) q^*(x_1|x_0)}{p_0(x_0) q(x_1|x_0)} q(x_0, x_1) dx_0 dx_1 = \\
& \int \log \frac{q^*(x_0, x_1)}{q(x_0, x_1)} q(x_0, x_1) dx_0 dx_1 = \\
& - \int \log \frac{q(x_0, x_1)}{q^*(x_0, x_1)} q(x_0, x_1) dx_0 dx_1 = -\text{KL}(q(x_0, x_1) \| q^*(x_0, x_1)).
\end{aligned}$$

Thus, $\text{KL}(q^* \| q) = -\text{KL}(q \| q^*)$. Since the KL divergence is non-negative, we derive that $q = q^*$.

Stage 2. In this stage, we prove the theorem itself. First, if $N > 1$, i.e., there is more than one intermediate time moment, we integrate $q(x_0, x_{t_1}, \dots, x_{t_N}, x_1)$ over all intermediate time moments except t_1 . On the one hand, we get

$$\begin{aligned}
q(x_0, x_{t_1}, x_1) &= \int q(x_0, x_{t_1}, \dots, x_{t_N}, x_1) dx_{t_2} \dots dx_{t_N} = \\
& \int p^{W^\epsilon}(x_{t_1}, \dots, x_{t_N} | x_0, x_1) q(x_0, x_1) dx_{t_2} \dots dx_{t_N} = p^{W^\epsilon}(x_{t_1} | x_0, x_1) q(x_1, x_0). \quad (17)
\end{aligned}$$

On the other hand, we derive

$$q(x_0, x_{t_1}, x_1) = \int q(x_0) q(x_{t_1} | x_0) \overbrace{\prod_{n=2}^{N+1} q(x_{t_n} | x_{t_{n-1}})}^{=q(x_{t_2}, \dots, x_{t_N}, x_1 | x_{t_1})} dx_{t_2} \dots dx_{t_N} = q(x_0) q(x_{t_1} | x_0) q(x_1 | x_{t_1}). \quad (18)$$

Combining (17) and (18) yields

$$q(x_0) q(x_{t_1} | x_0) q(x_1 | x_{t_1}) = q(x_0, x_{t_1}, x_1) = p^{W^\epsilon}(x_{t_1} | x_0, x_1) q(x_1, x_0). \quad (19)$$

Note that if $N = 1$, then we already have (19) from the conditions of the theorem. Therefore,

$$\begin{aligned}
p^{W^\epsilon}(x_{t_1} | x_0, x_1) q(x_1, x_0) &= q(x_0) q(x_{t_1} | x_0) q(x_1 | x_{t_1}) \\
p^{W^\epsilon}(x_{t_1} | x_0, x_1) q(x_1 | x_0) q(x_0) &= q(x_0) q(x_{t_1} | x_0) q(x_1 | x_{t_1}).
\end{aligned}$$

From now on, we are interested only in 3 time moments: $t_0 = 0$, t_1 and $t_{N+1} = 1$. To simplify the notation, we will write t instead of t_2 in the following proof. We take the logarithm and get

$$\log q(x_1 | x_0) = \log q(x_t | x_0) + \log q(x_1 | x_t) - \log p^{W^\epsilon}(x_t | x_0, x_1)$$

Then, we use the formula for the Brownian Bridge density:

$$\begin{aligned}
\log q(x_1|x_0) &= \log q(x_t|x_0) + \log q(x_1|x_t) - C + \frac{1}{2\epsilon t(1-t)} \|x_t - (tx_1 + (1-t)x_0)\|^2 = \\
&\quad \log q(x_t|x_0) + \log q(x_1|x_t) - C + \\
\frac{1}{2\epsilon t(1-t)} (\|x_t\|^2 + \|tx_1\|^2 + \|(1-t)x_0\|^2 - 2tx_t^T x_1 - 2(1-t)x_t^T x_0 + 2t(1-t)x_0^T x_1) &= \\
&\quad \log q(x_t|x_0) + \log q(x_1|x_t) - C + \\
\frac{\|x_t\|^2}{2\epsilon t(1-t)} + \frac{\|(1-t)x_0\|^2}{2\epsilon t(1-t)} + \frac{\|tx_1\|^2}{2\epsilon t(1-t)} - \frac{x_t^T x_1}{\epsilon(1-t)} - \frac{x_t^T x_0}{\epsilon t} + \frac{x_0^T x_1}{\epsilon} &= \\
\underbrace{\log q(x_1|x_t) + \frac{\|x_t\|^2}{2\epsilon t(1-t)} + \frac{\|tx_1\|^2}{2\epsilon t(1-t)} - \frac{x_t^T x_1}{\epsilon(1-t)}}_{\stackrel{\text{def}}{=} f_1(x_t, x_1)} - C + & \\
\underbrace{\frac{\|(1-t)x_0\|^2}{2\epsilon t(1-t)} + \log q(x_t|x_0) - \frac{x_t^T x_0}{\epsilon t} + \frac{x_0^T x_1}{\epsilon}}_{\stackrel{\text{def}}{=} f_2(x_t, x_0)}. &
\end{aligned}$$

Thus,

$$\begin{aligned}
\log q(x_1|x_0) &= f_1(x_t, x_1) + f_2(x_t, x_0) + \frac{x_0^T x_1}{\epsilon}, \\
\underbrace{\log q(x_1|x_0) - \frac{x_0^T x_1}{\epsilon}}_{\stackrel{\text{def}}{=} f_3(x_0, x_1)} &= f_1(x_t, x_1) + f_2(x_t, x_0), \\
f_3(x_0, x_1) &= f_1(x_t, x_1) + f_2(x_t, x_0). \tag{20}
\end{aligned}$$

Below, we prove that $f_3(x_0, x_1) = g_1(x_0) + g_2(x_1)$ for some functions g_1 and g_2 . We note that

$$f_3(x_0, 0) = f_1(x_t, 0) + f_2(x_t, x_0) \quad \Rightarrow \quad f_2(x_t, x_0) = f_3(x_0, 0) - f_1(x_t, 0). \tag{21}$$

We substitute (21) to (20):

$$\begin{aligned}
f_3(x_0, x_1) &= f_1(x_t, x_1) + \underbrace{f_3(x_0, 0) - f_1(x_t, 0)}_{= f_2(x_t, x_0)} \\
f_3(x_0, x_1) - f_3(x_0, 0) &= f_1(x_t, x_1) - f_1(x_t, 0). \tag{22}
\end{aligned}$$

Since there is no dependence on x_0 in the right part of (22), we conclude that $f_3(x_0, x_1) - f_3(x_0, 0)$ is a function of only x_1 . We define $g_1(x_1) \stackrel{\text{def}}{=} f_3(x_0, x_1) - f_3(x_0, 0)$ and $g_2(x_0) \stackrel{\text{def}}{=} f_3(x_0, 0)$. Now we have the desired result:

$$f_3(x_0, x_1) = g_1(x_1) + f_3(x_0, 0) = g_1(x_1) + g_2(x_0). \tag{23}$$

Thus,

$$f_3(x_0, x_1) = \log q(x_1|x_0) - \frac{x_0^T x_1}{\epsilon} = g_1(x_1) + g_2(x_0).$$

Now, we can use this result about the separation of variables together with the result from the first **stage** to conclude the proof of the theorem.

$$\begin{aligned}
\log q(x_1|x_0) &= g_1(x_1) + g_2(x_0) + \frac{x_0^T x_1}{\epsilon} = \\
g_1(x_1) + \frac{\|x_1\|^2}{2\epsilon} + g_2(x_0) + \frac{\|x_0\|^2}{2\epsilon} - \frac{\|x_0 - x_1\|^2}{2\epsilon}, & \\
q(x_1|x_0) &= \underbrace{\exp\left(g_2(x_0) + \frac{\|x_0\|^2}{2\epsilon}\right)}_{\stackrel{\text{def}}{=} C(x_0)} \exp\left(-\frac{\|x_0 - x_1\|^2}{2\epsilon}\right) \underbrace{\exp\left(g_1(x_1) + \frac{\|x_1\|^2}{2\epsilon}\right)}_{\stackrel{\text{def}}{=} \phi(x_1)} =
\end{aligned}$$

$$q(x_1|x_0) = C(x_0) \exp\left(-\frac{\|x_0 - x_1\|^2}{2\epsilon}\right) \phi(x_1),$$

$$q(x_0, x_1) = q(x_0)C(x_0) \exp\left(-\frac{\|x_0 - x_1\|^2}{2\epsilon}\right) \phi(x_1).$$

Hence, from the first **stage** of this proof it follows that $q(x_0, x_1)$ is the solution to the Static SB between $q(x_0) = p_0(x_0)$ and $q(x_1) = p_1(x_1)$ with the coefficient ϵ . That is, $p^{T^*}(x_0, x_1) = q(x_0, x_1)$. Since $q(x_{t_1}, \dots, x_{t_N}|x_0, x_1) = p^{W^\epsilon}(x_{t_1}, \dots, x_{t_N}|x_0, x_1)$ by the assumptions of the current theorem, we also conclude that $q(x_0, x_{t_1}, \dots, x_{t_N}, x_1) = p^{T^*}(x_0, x_{t_1}, \dots, x_{t_N}, x_1)$, i.e., the discrete processes coincide. \square

B.2 Proofs for Statements in Section 3.3

The logic of our justification of D-IMF for discrete processes generally follows the respective logic of the justification of IMF for continuous stochastic processes [43].

Proof of Proposition 3.3. The mild assumption here consists in the existence of at least one process $r \in \mathcal{R}(N)$ for which $\text{KL}(q||r) < \infty$. The reciprocal process $r \in \mathcal{R}(N)$ has its density in the form $r(x_0, x_{t_1}, \dots, x_{t_N}, x_1) = p^{W^\epsilon}(x_{t_1}, \dots, x_{t_N}|x_0, x_1)r(x_0, x_1)$ (see (7)). Thus, we need to optimize only the part $r(x_0, x_1)$. Below we show, that $r(x_0, x_1)$ should be equal $q(x_0, x_1)$ to minimize the functional.

$$\begin{aligned} \text{KL}(q||r) &= \int \log \frac{q(x_0, x_{\text{in}}, x_1)}{r(x_0, x_{\text{in}}, x_1)} q(x_0, x_{\text{in}}, x_1) dx_0 dx_{\text{in}} dx_1 = \\ &= \int \log \frac{q(x_{\text{in}}|x_0, x_1)q(x_0, x_1)}{\underbrace{r(x_{\text{in}}|x_0, x_1)}_{p^{W^\epsilon}(x_{\text{in}}|x_0, x_1)} r(x_0, x_1)} q(x_0, x_{\text{in}}, x_1) dx_0 dx_{\text{in}} dx_1 = \\ &= \underbrace{\int \log \frac{q(x_{\text{in}}|x_0, x_1)}{p^{W^\epsilon}(x_{\text{in}}|x_0, x_1)} q(x_0, x_{\text{in}}, x_1) dx_0 dx_{\text{in}} dx_1}_{=\text{Const}} + \int \log \frac{q(x_0, x_1)}{r(x_0, x_1)} q(x_0, x_{\text{in}}, x_1) dx_0 dx_{\text{in}} dx_1 = \\ &= \text{Const} + \underbrace{\int \log \frac{q(x_0, x_1)}{r(x_0, x_1)} q(x_0, x_1) dx_0 dx_1}_{=\text{KL}(q(x_0, x_1)||r(x_0, x_1))} = \text{Const} + \text{KL}(q(x_0, x_1)||r(x_0, x_1)) \end{aligned}$$

Hence, $\text{proj}_{\mathcal{R}}(q) = \arg \min_{r \in \mathcal{R}(N)} \text{KL}(q||r) = p^{W^\epsilon}(x_{\text{in}}|x_0, x_1)q(x_0, x_1)$. \square

Proof of Proposition 3.5. Similar to the previous proposition, the mild assumption here consists in the existence of at least one process $m \in \mathcal{M}(N)$ for which $\text{KL}(q||m) < \infty$. This proof is a bit more technical than for the reciprocal projection. We need to define new notation $x_{t_n, t_{n-1}}^{\text{not}} = (x_{t_0}, \dots, x_{t_{n-2}}, x_{t_{n+1}}, \dots, x_{t_{N+1}})$ for a vector of variables for all time moment except two time moments t_n and t_{n-1} .

$$\begin{aligned} \text{KL}(q||m) &= \int \log \frac{q(x_0, x_{\text{in}}, x_1)}{m(x_0, x_{\text{in}}, x_1)} q(x_0, x_{\text{in}}, x_1) dx_0 dx_{\text{in}} dx_1 = \\ &= \int \log \frac{q(x_0, x_{\text{in}}, x_1)}{m(x_0) \prod_{n=1}^{N+1} m(x_{t_n}|x_{t_{n-1}})} q(x_0, x_{\text{in}}, x_1) dx_0 dx_{\text{in}} dx_1 = \\ &= \int \log \frac{q(x_0)}{m(x_0)} q(x_0, x_{\text{in}}, x_1) dx_0 dx_{\text{in}} dx_1 + \int \log \frac{q(x_{\text{in}}, x_1|x_0)}{\prod_{n=1}^{N+1} m(x_{t_n}|x_{t_{n-1}})} q(x_0, x_{\text{in}}, x_1) dx_0 dx_{\text{in}} dx_1 = \\ &= \underbrace{\int \log \frac{q(x_0)}{m(x_0)} q(x_0) dx_0}_{\text{KL}(q(x_0)||m(x_0))} + \int \log \frac{q(x_{\text{in}}, x_1|x_0)}{\prod_{n=1}^{N+1} m(x_{t_n}|x_{t_{n-1}})} q(x_0, x_{\text{in}}, x_1) dx_0 = \end{aligned}$$

$$\text{KL}(q(x_0)||m(x_0)) + \int \log \frac{q(x_{\text{in}}, x_1|x_0)}{\prod_{n=1}^{N+1} m(x_{t_n}|x_{t_{n-1}})} q(x_0, x_{\text{in}}, x_1) dx_0 dx_{\text{in}} dx_1 + \quad (24)$$

$$\underbrace{N \int \log \frac{q(x_0, x_{\text{in}}, x_1)}{q(x_0, x_{\text{in}}, x_1)} q(x_0, x_{\text{in}}, x_1) dx_0 dx_{\text{in}} dx_1}_{=0} + \underbrace{\int \log \frac{q(x_0)}{q(x_0)} q(x_0, x_{\text{in}}, x_1) dx_0 dx_{\text{in}} dx_1}_{=0} = \quad (25)$$

$$\begin{aligned} & \text{KL}(q(x_0)||m(x_0)) + \int \log \frac{\prod_{n=1}^{N+1} q(x_0, x_{\text{in}}, x_1)}{\prod_{n=1}^{N+1} m(x_{t_n}|x_{t_{n-1}})} q(x_0, x_{\text{in}}, x_1) dx_0 dx_{\text{in}} dx_1 - \\ & (N \int \log q(x_0, x_{\text{in}}, x_1) q(x_0, x_{\text{in}}, x_1) dx_0 dx_{\text{in}} dx_1 + \int \log q(x_0) q(x_0) dx_0 dx_{\text{in}} dx_1) = \\ & \text{KL}(q(x_0)||m(x_0)) + \sum_{n=1}^{N+1} \int \log \frac{q(x_0, x_{\text{in}}, x_1)}{m(x_{t_n}|x_{t_{n-1}})} q(x_0, x_{\text{in}}, x_1) dx_0 dx_{\text{in}} dx_1 - \\ & (N \int \log q(x_0, x_{\text{in}}, x_1) q(x_0, x_{\text{in}}, x_1) dx_0 dx_{\text{in}} dx_1 + \int \log q(x_0) q(x_0) dx_0 dx_{\text{in}} dx_1) = \\ & \underbrace{\hspace{15em}}_{\stackrel{\text{def}}{=} C_1} \text{KL}(q(x_0)||m(x_0)) - C_1 + \\ & \sum_{n=1}^{N+1} \int \log \frac{q(x_{t_n}|x_{t_{n-1}}) q(x_{t_{n-1}}) q(x_{t_n}^{\text{not}}|x_{t_n}, x_{t_{n-1}})}{m(x_{t_n}|x_{t_{n-1}})} q(x_0, x_{\text{in}}, x_1) dx_0 dx_{\text{in}} dx_1 = \\ & \text{KL}(q(x_0)||m(x_0)) - C_1 + \underbrace{\sum_{n=1}^{N+1} \int \log (q(x_{t_{n-1}}) q(x_{t_n}^{\text{not}}|x_{t_n}, x_{t_{n-1}})) q(x_0, x_{\text{in}}, x_1) dx_0 dx_{\text{in}} dx_1}_{\stackrel{\text{def}}{=} C_2} \\ & \sum_{n=1}^{N+1} \int \log \frac{q(x_{t_n}|x_{t_{n-1}})}{m(x_{t_n}|x_{t_{n-1}})} q(x_0, x_{\text{in}}, x_1) dx_0 dx_{\text{in}} dx_1 = \\ & \text{KL}(q(x_0)||m(x_0)) + C_2 + \sum_{n=1}^{N+1} \underbrace{\left(\int \log \frac{q(x_{t_n}|x_{t_{n-1}})}{m(x_{t_n}|x_{t_{n-1}})} q(x_{t_n}|x_{t_{n-1}}) dx_{t_n} \right) q(x_{t_{n-1}}) dx_{t_{n-1}}}_{\text{KL}(q(x_{t_n}|x_{t_{n-1}})||m(x_{t_n}|x_{t_{n-1}}))} = \\ & \text{KL}(q(x_0)||m(x_0)) + \sum_{n=1}^{N+1} \int \text{KL}(q(x_{t_n}|x_{t_{n-1}})||m(x_{t_n}|x_{t_{n-1}})) q(x_{t_{n-1}}) dx_{t_{n-1}} + C_2. \end{aligned}$$

In the line (25), we add terms equal to zero, to match each $m(x_{t_n}|x_{t_{n-1}})$ by the separate term $q(x_0, x_{\text{in}}, x_1)$ in the line (25). We need it to as we want to place each term $m(x_{t_n}|x_{t_{n-1}})$ in the separate KL-divergence in the final expression. Hence, the minimizer of the objective $m^* \in \mathcal{M}(N)$ has $m^*(x_0) = q(x_0)$ and all transitional distributions $m^*(x_{t_n}|x_{t_{n-1}}) = q(x_{t_n}|x_{t_{n-1}})$, i.e. is given by

$$m^*(x_0, x_{\text{in}}, x_1) = [\text{proj}_{\mathcal{M}}(q)](x_0, x_{\text{in}}, x_1) = q(x_0) \prod_{n=1}^{N+1} q(x_{t_n}|x_{t_{n-1}}).$$

□

Proposition B.1. Assume that $r \in \mathcal{R}(N)$ and $m \in \mathcal{M}(N)$. If $\text{KL}(r||m) < \infty$ and $\text{KL}(r||\text{proj}_{\mathcal{M}}(r)) < \infty$, then

$$\text{KL}(r||m) = \text{KL}(r||\text{proj}_{\mathcal{M}}(r)) + \text{KL}(\text{proj}_{\mathcal{M}}(r)||m) \quad (26)$$

and if $\text{KL}(m||r) < \infty$, $\text{KL}(m||\text{proj}_{\mathcal{R}}(m)) < \infty$ then

$$\text{KL}(m||r) = \text{KL}(m||\text{proj}_{\mathcal{R}}(m)) + \text{KL}(\text{proj}_{\mathcal{R}}(m)||r)$$

Proof of Proposition B.1. Before proving the first equation (26) we prove the additional property of $r \in \mathcal{R}(N)$ for any $n \in [1, 2, \dots, N+1]$:

$$[\text{proj}_{\mathcal{M}} r](x_{t_n}, x_{t_{n-1}}) = r(x_{t_n}, x_{t_{n-1}}).$$

$$[\text{proj}_{\mathcal{M}}r](x_{t_n}, x_{t_{n-1}}) = [\text{proj}_{\mathcal{M}}r](x_{t_n} | x_{t_{n-1}}) [\text{proj}_{\mathcal{M}}r](x_{t_n}) = r(x_{t_n} | x_{t_{n-1}}) r(x_{t_n}). \quad (27)$$

Since $[\text{proj}_{\mathcal{M}}r](x_{t_n} | x_{t_{n-1}}) = r(x_{t_n} | x_{t_{n-1}})$ by the definition and since Markovian projection preserve all intermediate time marginals. Now we prove the first equation (26).

$$\begin{aligned} \text{KL}(r \| m) &= \int \log \frac{r(x_0, x_{\text{in}}, x_1)}{m(x_0, x_{\text{in}}, x_1)} r(x_0, x_{\text{in}}, x_1) dx_0 dx_{\text{in}} dx_1 = \\ &\quad \int \log \frac{r(x_0, x_{\text{in}}, x_1)}{m(x_0, x_{\text{in}}, x_1)} r(x_0, x_{\text{in}}, x_1) dx_0 dx_{\text{in}} dx_1 + \\ &\quad \underbrace{\int \log \frac{[\text{proj}_{\mathcal{M}}(r)](x_0, x_{\text{in}}, x_1)}{[\text{proj}_{\mathcal{M}}(r)](x_0, x_{\text{in}}, x_1)} r(x_0, x_{\text{in}}, x_1) dx_0 dx_{\text{in}} dx_1}_{=0} = \\ &\quad \underbrace{\int \log \frac{r(x_0, x_{\text{in}}, x_1)}{[\text{proj}_{\mathcal{M}}(r)](x_0, x_{\text{in}}, x_1)} r(x_0, x_{\text{in}}, x_1) dx_0 dx_{\text{in}} dx_1}_{\text{KL}(r \| \text{proj}_{\mathcal{M}}(r))} + \\ &\quad \int \log \frac{[\text{proj}_{\mathcal{M}}(r)](x_0, x_{\text{in}}, x_1)}{m(x_0, x_{\text{in}}, x_1)} r(x_0, x_{\text{in}}, x_1) dx_0 dx_{\text{in}} dx_1 = \\ \text{KL}(r \| \text{proj}_{\mathcal{M}}(r)) &+ \int \log \frac{[\text{proj}_{\mathcal{M}}(r)](x_0) \prod_{n=1}^{N+1} [\text{proj}_{\mathcal{M}}(r)](x_{t_n} | x_{t_{n-1}})}{m(x_0) \prod_{n=1}^{N+1} m(x_{t_n} | x_{t_{n-1}})} r(x_0, x_{\text{in}}, x_1) dx_0 dx_{\text{in}} dx_1 = \\ &\quad \text{KL}(r \| \text{proj}_{\mathcal{M}}(r)) + \text{KL}([\text{proj}_{\mathcal{M}}(r)](x_0) \| m(x_0)) + \\ &\quad \sum_{n=1}^{N+1} \int \log \frac{[\text{proj}_{\mathcal{M}}(r)](x_{t_n} | x_{t_{n-1}})}{m(x_{t_n} | x_{t_{n-1}})} r(x_0, x_{\text{in}}, x_1) dx_0 dx_{\text{in}} dx_1 = \\ &\quad \text{KL}(r \| \text{proj}_{\mathcal{M}}(r)) + \text{KL}([\text{proj}_{\mathcal{M}}(r)](x_0) \| m(x_0)) + \\ &\quad \sum_{n=1}^{N+1} \int \log \frac{[\text{proj}_{\mathcal{M}}(r)](x_{t_n} | x_{t_{n-1}})}{m(x_{t_n} | x_{t_{n-1}})} \underbrace{r(x_{t_n}, x_{t_{n-1}})}_{= [\text{proj}_{\mathcal{M}}(r)](x_{t_n}, x_{t_{n-1}})} dx_{t_n} dx_{t_{n-1}} = \\ &\quad \text{KL}(r \| \text{proj}_{\mathcal{M}}(r)) + \text{KL}([\text{proj}_{\mathcal{M}}(r)](x_0) \| m(x_0)) + \\ &\quad \sum_{n=1}^{N+1} \int \log \frac{[\text{proj}_{\mathcal{M}}(r)](x_{t_n} | x_{t_{n-1}})}{m(x_{t_n} | x_{t_{n-1}})} [\text{proj}_{\mathcal{M}}(r)](x_{t_n}, x_{t_{n-1}}) dx_{t_n} dx_{t_{n-1}} = \\ &\quad \text{KL}(r \| \text{proj}_{\mathcal{M}}(r)) + \text{KL}([\text{proj}_{\mathcal{M}}(r)](x_0) \| m(x_0)) + \\ &\quad \sum_{n=1}^{N+1} \int \log \frac{[\text{proj}_{\mathcal{M}}(r)](x_{t_n} | x_{t_{n-1}})}{m(x_{t_n} | x_{t_{n-1}})} [\text{proj}_{\mathcal{M}}(r)](x_0, x_{\text{in}}, x_1) dx_0 dx_{\text{in}} dx_1 = \\ &\quad \text{KL}(r \| \text{proj}_{\mathcal{M}}(r)) + \underbrace{\int \log \frac{[\text{proj}_{\mathcal{R}}](q)(x_0)}{m(x_0)} [\text{proj}_{\mathcal{R}}](q)(x_0) dx_0}_{= \text{KL}([\text{proj}_{\mathcal{M}}(r)](x_0) \| m(x_0))} + \\ &\quad \int \log \frac{\prod_{n=1}^{N+1} [\text{proj}_{\mathcal{M}}(r)](x_{t_n} | x_{t_{n-1}})}{\prod_{n=1}^{N+1} m(x_{t_n} | x_{t_{n-1}})} [\text{proj}_{\mathcal{M}}(r)](x_0, x_{\text{in}}, x_1) dx_0 dx_{\text{in}} dx_1 = \\ \text{KL}(r \| \text{proj}_{\mathcal{M}}(r)) &+ \underbrace{\int \log \frac{[\text{proj}_{\mathcal{M}}(r)](x_0, x_{\text{in}}, x_1)}{m(x_0, x_{\text{in}}, x_1)} [\text{proj}_{\mathcal{M}}(r)](x_0, x_{\text{in}}, x_1) dx_0 dx_{\text{in}} dx_1}_{\text{KL}(\text{proj}_{\mathcal{M}}(r) \| m)} = \\ &\quad \text{KL}(r \| \text{proj}_{\mathcal{M}}(r)) + \text{KL}(\text{proj}_{\mathcal{M}}(r) \| m). \end{aligned}$$

That concludes the proof of the first equation (26). The proof for the second equation (27) is similar.

$$\text{KL}(m \| r) = \int \log \frac{m(x_0, x_{\text{in}}, x_1)}{r(x_0, x_{\text{in}}, x_1)} m(x_0, x_{\text{in}}, x_1) dx_0 dx_{\text{in}} dx_1 +$$

$$\begin{aligned}
& \int \log \underbrace{\frac{[\text{proj}_{\mathcal{R}}(m)](x_0, x_{\text{in}}, x_1)}{[\text{proj}_{\mathcal{R}}(m)](x_0, x_{\text{in}}, x_1)}}_{=0}} m(x_0, x_{\text{in}}, x_1) dx_0 dx_{\text{in}} dx_1 = \\
& \underbrace{\int \log \frac{m(x_0, x_{\text{in}}, x_1)}{[\text{proj}_{\mathcal{R}}(m)](x_0, x_{\text{in}}, x_1)} m(x_0, x_{\text{in}}, x_1) dx_0 dx_{\text{in}} dx_1}_{\text{KL}(m \parallel \text{proj}_{\mathcal{R}}(m))} + \\
& \int \log \frac{[\text{proj}_{\mathcal{R}}(m)](x_0, x_{\text{in}}, x_1)}{r(x_0, x_{\text{in}}, x_1)} m(x_0, x_{\text{in}}, x_1) dx_0 dx_{\text{in}} dx_1 = \\
& \text{KL}(m \parallel \text{proj}_{\mathcal{R}}(m)) + \\
& \int \log \frac{p^{W_\epsilon}(x_{\text{in}}|x_0, x_1) [\text{proj}_{\mathcal{R}}(m)](x_0, x_1)}{p^{W_\epsilon}(x_{\text{in}}|x_0, x_1) r(x_0, x_1)} m(x_0, x_{\text{in}}, x_1) dx_0 dx_{\text{in}} dx_1 = \\
& \int \log \frac{[\text{proj}_{\mathcal{R}}(m)](x_0, x_1)}{r(x_0, x_1)} \underbrace{m(x_0, x_1)}_{=[\text{proj}_{\mathcal{R}}(m)](x_0, x_1)} dx_0 dx_1 = \\
& \text{KL}(m \parallel \text{proj}_{\mathcal{R}}(m)) + \int \log \frac{[\text{proj}_{\mathcal{R}}(m)](x_0, x_1)}{r(x_0, x_1)} [\text{proj}_{\mathcal{R}}(m)](x_0, x_1) dx_0 dx_1 = \\
& \text{KL}(m \parallel \text{proj}_{\mathcal{R}}(m)) + \int \log \frac{[\text{proj}_{\mathcal{R}}(m)](x_0, x_1)}{r(x_0, x_1)} [\text{proj}_{\mathcal{R}}(m)](x_0, x_{\text{in}}, x_1) dx_0 dx_{\text{in}} dx_1 = \\
& \text{KL}(m \parallel \text{proj}_{\mathcal{R}}(m)) + \int \log \frac{p^{W_\epsilon}(x_{\text{in}}|x_0, x_1) [\text{proj}_{\mathcal{R}}(m)](x_0, x_1)}{p^{W_\epsilon}(x_{\text{in}}|x_0, x_1) r(x_0, x_1)} [\text{proj}_{\mathcal{R}}(m)](x_0, x_{\text{in}}, x_1) dx_0 dx_{\text{in}} dx_1 = \\
& \text{KL}(m \parallel \text{proj}_{\mathcal{R}}(m)) + \underbrace{\int \log \frac{[\text{proj}_{\mathcal{R}}(m)](x_0, x_{\text{in}}, x_1)}{r(x_0, x_{\text{in}}, x_1)} [\text{proj}_{\mathcal{R}}(m)](x_0, x_{\text{in}}, x_1) dx_0 dx_{\text{in}} dx_1}_{=\text{KL}([\text{proj}_{\mathcal{R}}(m)](x_0, x_{\text{in}}, x_1) \parallel r(x_0, x_{\text{in}}, x_1))} \\
& = \text{KL}(m \parallel \text{proj}_{\mathcal{R}}(m)) + \text{KL}(\text{proj}_{\mathcal{R}}(m) \parallel r)
\end{aligned}$$

That concludes the proof of the second equation (27). \square

Proposition B.2. *Assume that we have a sequence of processes $\{q^l\}_{l=0}^\infty$ from D-IMF procedure starting from q^0 for which $\text{KL}(q^0 \parallel q^*) < \infty$. Assume that for each reciprocal and Markovian projection in a sequence $\text{KL}(q^l \parallel q^{l+1}) < \infty$. Then $\text{KL}(q^{l+1} \parallel q^*) \leq \text{KL}(q^l \parallel q^*)$ and $\lim_{l \rightarrow \infty} \text{KL}(q^l \parallel q^{l+1}) = 0$.*

Proof of Proposition B.2. We use the same technique as was used in the proof of IMF procedure [43, Proposition 7], and for forward KL in [39]. We apply Proposition B.1 and for every l we have:

$$\text{KL}(q^l \parallel q^*) = \text{KL}(q^l \parallel q^{l+1}) + \text{KL}(q^{l+1} \parallel q^*)$$

Since the KL divergence is non-negative, it follows that $\text{KL}(q^{l+1} \parallel q^*) \leq \text{KL}(q^l \parallel q^*)$. Applying this proposition for each $l \leq L \in \mathbb{N}$, we have

$$\text{KL}(q^0 \parallel q^*) = \text{KL}(q^0 \parallel q^1) + \text{KL}(q^1 \parallel q^*) = \sum_{l=0}^L \text{KL}(q^l \parallel q^{l+1}) + \text{KL}(q^{L+1} \parallel q^*).$$

Since the KL divergence is non-negative and $\text{KL}(q^0 \parallel q^*) < \infty$, it follows that $\lim_{l \rightarrow \infty} \text{KL}(q^l \parallel q^{l+1}) = 0$. \square

Proof of Theorem 3.6. The mild assumptions here are the assumptions of the Proposition B.2, i.e. $\text{KL}(q^l \parallel q^{l+1}) < \infty$.

We follow the proof of [43, Theorem 8] but do the derivations for discrete stochastic processes instead of continuous. By the previous Proposition B.2 it holds that $\text{KL}(q^l \parallel q^*) \leq \text{KL}(q^0 \parallel q^*) < \infty$ for every l . Hence the sequence $(q^l)_{l=0}^\infty$ and its subsequences of markovian $(m^l)_{l=1}^\infty = (q^{2l+1})_{l=1}^\infty$ and reciprocal processes $(r^l)_{l=1}^\infty = (q^{2l})_{l=1}^\infty$ are subsets of a compact set $\{q \in \mathcal{P}_{2,ac}(\mathbb{R}^{D \times (N+2)})\}$:

$\text{KL}(q\|q^*) \leq \text{KL}(q^0\|q^*)$ [46, Theorem 20]. Hence, $(m_l)_{l=1}^\infty$ contains a convergent subsequence $(m^{l_k})_{k=1}^\infty \rightarrow m^*$ and $(r^{l_k})_{k=1}^\infty$ contains a convergent subsequence $(r^{l_{k_j}})_{j=1}^\infty \rightarrow r^*$. Since sets of Markovian $\mathcal{M}(N)$ and reciprocal $\mathcal{R}(N)$ processes are closed under weak convergence $m^* \in \mathcal{M}(N)$ and $r^* \in \mathcal{R}(N)$. From the lower semicontinuity of KL divergence in the weak topology [46, Theorem 19] and $\lim_{l \rightarrow \infty} \text{KL}(q^l\|q^{l+1}) = 0$ (see Proposition B.2):

$$0 \leq \text{KL}(m^*\|r^*) \leq \liminf_{k \rightarrow \infty} \text{KL}\left(\left(m^{l_{k_j}}\right)_{j=0}^\infty \left\| \left(r^{l_{k_j}}\right)_{j=0}^\infty\right.\right) = 0. \quad (28)$$

Thus, $m^* = r^* \stackrel{\text{def}}{=} q^{\text{lim}}$. We know that q^{lim} has the same marginals $p_0(x_0) = q(x_0)$ and $p_1(x_1) = q(x_1)$ since both Markovian and reciprocal projections preserve marginals. By Theorem 3.1 since $q^{\text{lim}} \in \mathcal{M}(N) \cap \mathcal{R}(N)$, then $q^{\text{lim}}(x_0, x_{\text{in}}, x_1) = p^{T^*}(x_0, x_{\text{in}}, x_1)$. Finally, $\lim_{k \rightarrow \infty} \text{KL}(q^l(x_0, x_{\text{in}}, x_1)\|p^{T^*}(x_0, x_{\text{in}}, x_1)) = 0$ follows using $\lim_{j \rightarrow \infty} \text{KL}\left(r^{l_{k_j}}(x_0, x_{\text{in}}, x_1)\|p^{T^*}(x_0, x_{\text{in}}, x_1)\right) = 0$ and the monotonicity of $\text{KL}(q^l\|q^*)$ (Proposition B.2). \square

B.3 Proofs of the Statements in §3.4

The proofs in this subsection are the most technical as there are a lot of manipulations with matrices.

Proof of Theorem 3.7. From (6) and (5) follows that the discrete Brownian Bridge $p^{W^\epsilon}(x_{\text{in}}|x_0, x_1)$ has also a Gaussian distribution. The covariance of the Brownian Bridge with coefficient ϵ at times $s < t$ [16][Eq. 9.14] is $\epsilon s(1-t)$. Thus, the matrix ϵK is a covariance matrix for all pairs of time moments $t, t' \in [t_1, \dots, t_N]$ of the considered discrete Brownian Bridge $p^{W^\epsilon}(x_{\text{in}}|x_0, x_1)$. The mean value $\mathbb{E}[x_{t_n}|x_0, x_1]$ of Brownian Bridge at time t_n is equal to $t_n x_1 + (1-t_n)x_0$. Thus, the discrete Brownian Bridge has the following distribution $p^{W^\epsilon}(x_{\text{in}}|x_0, x_1) = \mathcal{N}(x_{\text{in}}|Ux_{01}, \epsilon K)$.

The reciprocal projection is given by:

$$[\text{proj}_{\mathcal{R}}q](x_{\text{in}}, x_0, x_1) = p^{W^\epsilon}(x_{\text{in}}|x_0, x_1)q(x_0, x_1). \quad (29)$$

Since it is a product of two Gaussian distributions, our goal is to find the mean vector and covariance matrix of $[\text{proj}_{\mathcal{R}}q](x_{\text{in}}, x_0, x_1)$.

The mean vector value of $[\text{proj}_{\mathcal{R}}q](x_{\text{in}}, x_0, x_1)$ for each t_n is given by

$$\mathbb{E}x_n = \int \mathbb{E}[x_{t_n}|x_0, x_1]q(x_0, x_1)dx_0x_1 = t_n\mu_1 + (1-t_n)\mu_0,$$

where μ_0 and μ_1 are means of $q(x_0)$ and $q(x_1)$. Thus, the mean vector of $[\text{proj}_{\mathcal{R}}q](x_{\text{in}}, x_0, x_1)$ is $(U\mu_{01}, \mu_0, \mu_1)$.

Now, we need to find the covariance matrix Σ_R . We first will find the inverse of the covariance matrix

$$\Sigma_R^{-1} = \begin{pmatrix} A & B \\ B^T & C \end{pmatrix}$$

of $[\text{proj}_{\mathcal{R}}q](x_{\text{in}}, x_0, x_1)$. Here A has shape $ND \times ND$ as the matrix K , while the matrix C has the shape $2D \times 2D$ as the matrix Σ . Matrices A and C are symmetric since they are a part of the inversed symmetric matrix Σ_R . We exploit the fact that the logarithm of a Gaussian distribution has the form:

$$\begin{aligned} \log([\text{proj}_{\mathcal{R}}q](x_{\text{in}}, x_0, x_1)) &= \\ \log C - \frac{1}{2}((x_{\text{in}}, x_{01}) - (U\mu_{01}, \mu_{01}))^T \Sigma_R^{-1} ((x_{\text{in}}, x_{01}) - (U\mu_{01}, \mu_{01})) &= \\ \log C - \frac{1}{2}((x_{\text{in}}, x_{01}) - (U\mu_{01}, \mu_{01}))^T \begin{pmatrix} A & B \\ B^T & C \end{pmatrix} ((x_{\text{in}}, x_{01}) - (U\mu_{01}, \mu_{01})) &= \\ \log C - \frac{1}{2}(x_{\text{in}} - U\mu_{01})^T A (x_{\text{in}} - U\mu_{01}) - \frac{1}{2}(x_{01} - \mu_{01})^T C (x_{01} - \mu_{01}) + & \\ (x_{\text{in}} - U\mu_{01})^T B (x_{01} - \mu_{01}). & \end{aligned}$$

In turn, from the (29) we have:

$$\begin{aligned}
& \log([\text{proj}_{\mathcal{R}}q](x_{\text{in}}, x_0, x_1)) = \log p^{W^\epsilon}(x_{\text{in}}|x_0, x_1) + \log q(x_0, x_1) = \\
& \log C - \frac{1}{2}(x_{\text{in}} - Ux_{01})^T(\epsilon K)^{-1}(x_{\text{in}} - Ux_{01}) - \frac{1}{2}(x_{01} - \mu_{01})^T \Sigma^{-1}(x_{01} - \mu_{01}) = \\
& \log C - \frac{1}{2}x_{\text{in}}^T(\epsilon K)^{-1}x_{\text{in}} + x_{\text{in}}^T(\epsilon K)^{-1}Ux_{01} - \frac{1}{2}(Ux_{01})^T(\epsilon K)^{-1}Ux_{01} - \\
& \quad \frac{1}{2}x_{01}^T \Sigma^{-1}x_{01} + x_{01}^T \Sigma^{-1}\mu_{01} - \frac{1}{2}\mu_{01}^T \Sigma^{-1}\mu_{01} = \\
& \log C - \frac{1}{2}x_{\text{in}}^T \underbrace{(\epsilon K)^{-1}}_{=A} x_{\text{in}} + x_{\text{in}}^T \underbrace{(\epsilon K)^{-1}U}_{=B} x_{01} - \frac{1}{2}x_{01}^T \underbrace{(U^T(\epsilon K)^{-1}U + \Sigma^{-1})}_{=C} x_{01} + \\
& \quad x_{01}^T \Sigma^{-1}\mu_{01} - \frac{1}{2}\mu_{01}^T \Sigma^{-1}\mu_{01}.
\end{aligned}$$

By matching the formulas above, it follows:

$$A = (\epsilon K)^{-1}, \quad B = -(\epsilon K)^{-1}U, \quad C = U^T(\epsilon K)^{-1}U + \Sigma^{-1}. \quad (30)$$

Thus, we have:

$$\Sigma_R^{-1} = \begin{pmatrix} A & B \\ B^T & C \end{pmatrix} = \begin{pmatrix} (\epsilon K)^{-1} & -(\epsilon K)^{-1}U \\ -((\epsilon K)^{-1}U)^T & U^T(\epsilon K)^{-1}U + \Sigma^{-1} \end{pmatrix}$$

By using the formula of block-wise matrix inversion:

$$\begin{pmatrix} A & B \\ B^T & C \end{pmatrix}^{-1} = \begin{pmatrix} A^{-1} + A^{-1}B(C - B^T A^{-1}B)^{-1}B^T A^{-1} & -A^{-1}B(C - B^T A^{-1}B)^{-1} \\ -(C - B^T A^{-1}B)^{-1}B^T A^{-1} & (C - B^T A^{-1}B)^{-1} \end{pmatrix}. \quad (31)$$

Applying this formula, we have:

$$\begin{aligned}
(C - B^T A^{-1}B)^{-1} &= (U^T(\epsilon K)^{-1}U + \Sigma^{-1} - U^T(\epsilon K)^{-1}(\epsilon K)(\epsilon K)^{-1}U)^{-1} = (\Sigma^{-1})^{-1} = \Sigma. \\
A^{-1} + A^{-1}B(C - B^T A^{-1}B)^{-1}B^T A^{-1} &= \\
& \epsilon K + \epsilon K(\epsilon K)^{-1}U\Sigma\Sigma^{-1}\Sigma U^T \epsilon K(\epsilon K)^{-1} = \epsilon K + U\Sigma U^T. \\
-A^{-1}B(C - B^T A^{-1}B)^{-1} &= -\epsilon K(\epsilon K)^{-1}U\Sigma = U\Sigma.
\end{aligned}$$

Thus, we obtain the desired result:

$$\Sigma_R = \begin{pmatrix} \epsilon K + U\Sigma U^T & U\Sigma \\ (U\Sigma)^T & \Sigma \end{pmatrix}.$$

□

Proof of Theorem 3.8. First, since from the condition of the theorem $q(x_{\text{in}}, x_0, x_1)$ has Gaussian distribution, it follows that joint distribution of two time moments $q(x_{t_n}, x_{t_{n-1}})$ is also Gaussian and is given by:

$$q(x_{t_n}, x_{t_{n-1}}) = \mathcal{N}\left(\begin{pmatrix} x_{t_n} \\ x_{t_{n-1}} \end{pmatrix} \middle| \begin{pmatrix} \mu_{t_n} \\ \mu_{t_{n-1}} \end{pmatrix}, \begin{pmatrix} (\tilde{\Sigma}_R)_{t_n, t_n} & (\tilde{\Sigma}_R)_{t_n, t_{n-1}} \\ (\tilde{\Sigma}_R)_{t_{n-1}, t_n} & (\tilde{\Sigma}_R)_{t_{n-1}, t_{n-1}} \end{pmatrix}\right) \quad (32)$$

Here $(\tilde{\Sigma}_R)_{t_i, t_j}$ represent submatrix of $\tilde{\Sigma}_R$ with covariance of x_{t_i} and x_{t_j} . Hence, the conditional distributions are given by [34, Sec 8.1.3]:

$$\begin{aligned}
q(x_{t_n} | x_{t_{n-1}}) &= \mathcal{N}(x_{t_n} | \hat{\mu}_{t_n}(x_{t_{n-1}}), \hat{\Sigma}_{t_n}), \\
\hat{\mu}_{t_n}(x_{t_{n-1}}) &\stackrel{\text{def}}{=} \mu_{t_n} + (\tilde{\Sigma}_R)_{t_n, t_{n-1}}((\tilde{\Sigma}_R)_{t_{n-1}, t_{n-1}})^{-1}(x_{t_{n-1}} - \mu_{t_{n-1}}), \\
\hat{\Sigma}_{t_n} &\stackrel{\text{def}}{=} (\tilde{\Sigma}_R)_{t_n, t_n} - (\tilde{\Sigma}_R)_{t_n, t_{n-1}}((\tilde{\Sigma}_R)_{t_{n-1}, t_{n-1}})^{-1}((\tilde{\Sigma}_R)_{t_n, t_{n-1}})^T.
\end{aligned}$$

That concludes the first part of our proof about the whole distribution $[\text{proj}_{\mathcal{M}}q](x_0, x_{\text{in}}, x_1)$ of Markovian projection. Next we find the distribution of $[\text{proj}_{\mathcal{M}}q](x_0, x_1)$. We consider the sequence

$[\text{proj}_{\mathcal{M}}q](x_{t_n}|x_0)$ for $n \in [1, \dots, N+1]$. We already know the expression for $n=1$ which is given by $[\text{proj}_{\mathcal{M}}q](x_{t_1}|x_0) = q(x_{t_1}|x_0)$ above. For other n , we use the following expression:

$$[\text{proj}_{\mathcal{M}}q](x_{t_n}|x_0) = \int q(x_{t_n}|x_{t_{n-1}})[\text{proj}_{\mathcal{M}}q](x_{t_{n-1}}|x_0)dx_{t_{n-1}} \quad (33)$$

Since the process $q(x_0, x_{\text{in}}, x_1)$ has a Gaussian distribution, then all its joint and conditional distributions are also Gaussian. Hence, we only need to compute the mean $\tilde{\mu}_{t_n}(x_0)$ and variance $\tilde{\Sigma}_{t_n}$ of $[\text{proj}_{\mathcal{M}}q](x_{t_n}|x_0) = \mathcal{N}(x_{t_n}|\tilde{\mu}_{t_n}(x_0), \tilde{\Sigma}_{t_n})$ in (33). First, we compute mean $\tilde{\mu}_{t_n}(x_0)$ by using the properties of conditional expectations.

$$\begin{aligned} \tilde{\mu}_{t_n}(x_0) &= \int \hat{\mu}_{t_n}(x_{t_{n-1}})[\text{proj}_{\mathcal{M}}q](x_{t_{n-1}}|x_0)dx_{t_{n-1}} = \\ &= \mu_{t_n} + (\tilde{\Sigma}_R)_{t_n, t_{n-1}}((\tilde{\Sigma}_R)_{t_{n-1}, t_{n-1}})^{-1} \left(\int x_{t_{n-1}} q(x_{t_{n-1}}|x_0)dx_{t_{n-1}} - \mu_{t_{n-1}} \right) = \\ &= \mu_{t_n} + \underbrace{(\Sigma_R)_{t_n, t_{n-1}}((\Sigma_R)_{t_{n-1}, t_{n-1}})^{-1}}_{\stackrel{\text{def}}{=} B_{t_n}} (\tilde{\mu}_{t_{n-1}}(x_0) - \mu_{t_{n-1}}) = \hat{\mu}_{t_n}(\tilde{\mu}_{t_{n-1}}(x_0)) \end{aligned}$$

Then we compute $\tilde{\Sigma}_{t_n}$ by using the law of total variance:

$$\begin{aligned} \tilde{\Sigma}_{t_n} &= \text{Var}_{[\text{proj}_{\mathcal{M}}q](x_{t_n}|x_0)} x_{t_n} = \\ &= \mathbb{E}_{[\text{proj}_{\mathcal{M}}q](x_{t_{n-1}}|x_0)} (\text{Var}_{q(x_{t_n}|x_{t_{n-1}})} x_{t_n}) + \text{Var}_{[\text{proj}_{\mathcal{M}}q](x_{t_{n-1}}|x_0)} (\mathbb{E}_{q(x_{t_n}|x_{t_{n-1}})} x_{t_n}). \end{aligned}$$

Since $\text{Var}_{q(x_{t_n}|x_{t_{n-1}})} x_{t_n} = \hat{\Sigma}_{t_n}$ is a constant, we have $\mathbb{E}_{[\text{proj}_{\mathcal{M}}q](x_{t_{n-1}}|x_0)} (\text{Var}_{q(x_{t_n}|x_{t_{n-1}})} x_{t_n}) = \hat{\Sigma}_{t_n}$. As for the second term, we have

$$\begin{aligned} \mathbb{E}_{q(x_{t_n}|x_{t_{n-1}})} x_{t_n} &= \hat{\mu}_{t_n}(x_{t_{n-1}}) = \\ &= \mu_{t_n} + (\tilde{\Sigma}_R)_{t_n, t_{n-1}}((\tilde{\Sigma}_R)_{t_{n-1}, t_{n-1}})^{-1} (x_{t_{n-1}} - \mu_{t_{n-1}}), \end{aligned}$$

where $x_{t_{n-1}} \sim [\text{proj}_{\mathcal{M}}q](x_{t_{n-1}}|x_0)$. Hence $\mathbb{E}_{q(x_{t_n}|x_{t_{n-1}})} x_{t_n}$ is a linear transformation of a random variable $x_{t_{n-1}}$ with the Gaussian distribution $[\text{proj}_{\mathcal{M}}q](x_{t_{n-1}}|x_0)$ with the variance of $\mathbb{E}_{q(x_{t_n}|x_{t_{n-1}})} x_{t_n}$ is given by:

$$\begin{aligned} \text{Var}_{[\text{proj}_{\mathcal{M}}q](x_{t_{n-1}}|x_0)} (\mathbb{E}_{q(x_{t_n}|x_{t_{n-1}})} x_{t_n}) &= \\ (\tilde{\Sigma}_R)_{t_n, t_{n-1}}((\tilde{\Sigma}_R)_{t_{n-1}, t_{n-1}})^{-1} (\tilde{\Sigma}_R)_{t_n} ((\tilde{\Sigma}_R)_{t_{n-1}, t_{n-1}})^{-1} ((\tilde{\Sigma}_R)_{t_n, t_{n-1}})^T &= \hat{\Sigma}_{t_n} + B_{t_n} (\tilde{\Sigma}_R)_{t_n} B_{t_n}^T. \end{aligned}$$

Thus, we finally have:

$$\tilde{\Sigma}_{t_n} = \hat{\Sigma}_{t_n} + B_{t_n} (\tilde{\Sigma}_R)_{t_n} B_{t_n}^T.$$

Now we can derive the $[\text{proj}_{\mathcal{M}}q](x_0, x_1)$, which is given by

$$[\text{proj}_{\mathcal{M}}q](x_0, x_1) = [\text{proj}_{\mathcal{M}}q](x_1|x_0)q(x_0).$$

To do it, we use the same approach that we used for computing $p^{W^\epsilon}(x_{\text{in}}|x_0, x_1)q(x_0, x_1)$ in the previous proof. This time, we have:

$$A = \tilde{\Sigma}_{t_n}^{-1}, \quad B = -\tilde{\Sigma}_{t_n}^{-1} \left(\prod_{n=1}^{N+1} B_{t_n} \right), \quad C = \left(\prod_{n=1}^{N+1} B_{t_n} \right)^T \tilde{\Sigma}_{t_n}^{-1} \left(\prod_{n=1}^{N+1} B_{t_n} \right) + \Sigma_0^{-1}$$

Hence, after a similar matrix inversion, we have a covariance between x_0 and x_1 as:

$$\Sigma_{01} = \left(\prod_{n=1}^{N+1} B_{t_n} \right) \Sigma_0, \quad (34)$$

while the covariances between x_0 and x_1 with themselves are Σ_0 and Σ_1 since markovian projection preserves the marginals of the distribution, i.e.:

$$[\text{proj}_{\mathcal{M}}q](x_0, x_1) = \mathcal{N} \left(\begin{pmatrix} x_0 \\ x_1 \end{pmatrix} \middle| \begin{pmatrix} \mu_0 \\ \mu_1 \end{pmatrix}, \begin{pmatrix} \Sigma_0 & \Sigma_{01} \\ (\Sigma_{01})^T & \Sigma_1 \end{pmatrix} \right), \quad \Sigma_{01} = \prod_{n=1}^{N+1} \underbrace{(\Sigma_R)_{t_n, t_{n-1}}((\Sigma_R)_{t_{n-1}, t_{n-1}})^{-1}}_{=B_{t_n}} \Sigma_0.$$

□

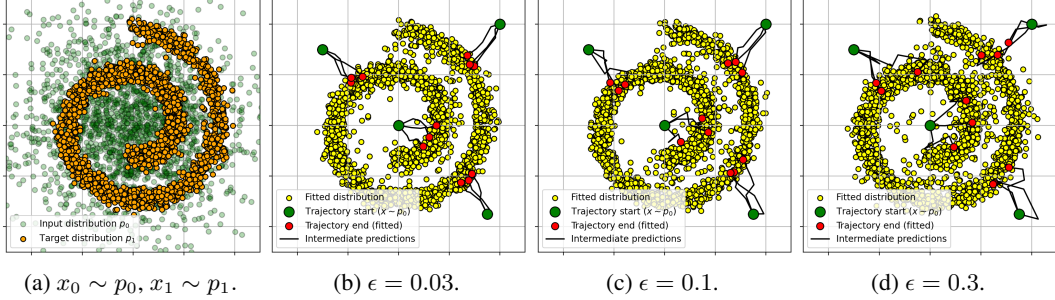


Figure 4: The final process q_θ learned with ASBM (ours) in *Gaussian* \rightarrow *Swiss roll* example.

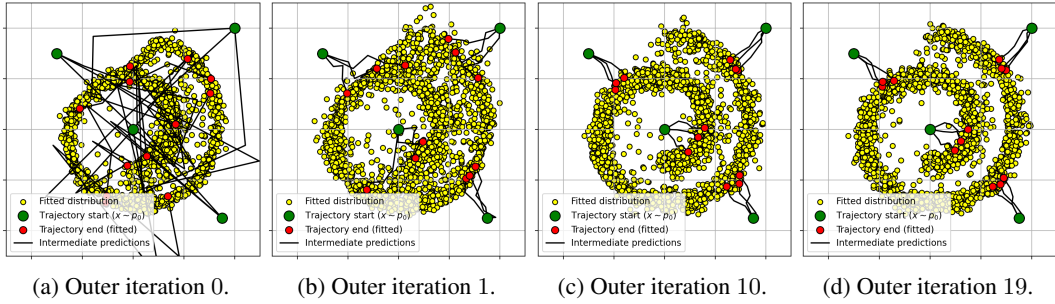


Figure 5: Evolution of our learned discrete process q_θ depending on D-IMF iteration in *Gaussian* \rightarrow *Swiss roll* example with $\epsilon = 0.03$.

C Additional Experiments

C.1 Illustrative 2D Example

Here we consider the SB problem with p_0 as a 2D Gaussian distribution and p_1 as the Swiss-roll distribution. We use independent $q^0(x_0, x_1) = p_0(x_0)p_1(x_1)$, $N = 3$ ($t_n = \frac{n}{N+1}$) and $K = 20$ outer iterations. We run our ASBM algorithm with different values of parameter ϵ and present our results in Figure 4. In all the cases, we observe the convergence to the target distribution. Overall, the trajectories are similar to the Brownian bridge and the closeness of start and endpoints is preserved. In Figure 5 we show the evolution of trajectories for different D-IMF iterations, which become more straight when number of iterations increase.

C.2 Benchmark

We use the SB mixtures benchmark proposed by [13, §4] to experimentally verify that our ASBM algorithm is indeed able to solve the Schrödinger Bridge between p_0 and p_1 . The benchmark provides continuous probability distribution pairs p_0, p_1 for dimensions $D \in \{2, 16, 64, 128\}$ with the known static SB solution $p^{T^*}(x_0, x_1)$ for parameters $\epsilon \in \{0.1, 1.10\}$. To evaluate the quality of our recovered SB solution, we use cBW_2^2 -UVP metric as suggested by the authors [13, §5] and provide results in Table 1. Additionally, we study how our approach learns the target distribution p_1 in Table 2. In all the cases, we run our ASBM algorithm starting from the independent coupling between p_0 and p_1 .

As the baselines, we consider other neural bridge matching methods [45, 43]. The first one (SF²M-Sink) is based on minibatch OT approximations, while the latter implements continuous IMF (DSBM). Additionally, we include the results of the best algorithm (for each setup) from the benchmark paper [13].

As shown in the Table 1, our algorithm demonstrates superior performance on $\epsilon = 10$, superior performance or comparable performance on $\epsilon = 1$, slightly worse performance w.r.t. SF²M-Sink [45] and superior performance w.r.t. DSBM [43] on $\epsilon = 0.1$. Also, from Table 2 one may note that ASBM fits target distribution better than other Bridge Matching SB algorithms.

		$\epsilon = 0.1$				$\epsilon = 1$				$\epsilon = 10$				
Algorithm Type		$D=2$	$D=16$	$D=64$	$D=128$	$D=2$	$D=16$	$D=64$	$D=128$	$D=2$	$D=16$	$D=64$	$D=128$	
Best algorithm on benchmark [†]		Varies	1.94	13.67	11.74	11.4	1.04	9.08	18.05	15.23	1.40	1.27	2.36	1.31
	DSBM [†]	5.2	16.8	37.3	35	0.3	1.1	9.7	31	3.7	105	3557	15000	
	SF ² M-Sink [†]	0.54	3.7	9.5	10.9	0.2	1.1	9	23	0.31	4.9	319	819	
	ASBM (ours)	0.89	8.2	13.5	53.7	0.19	1.6	5.8	10.5	0.13	0.4	1.9	4.7	

Table 1: Comparisons of $c\text{BW}_2^2$ -UVP \downarrow (%) between the static SB solution $p^T(x_0, x_1)$ and the learned $q_\theta(x_0, x_1)$ on the SB benchmark. The best metric over *bridge Matching algorithms* is **bolded**. Results marked with [†] are taken from [11].

		$\epsilon = 0.1$				$\epsilon = 1$				$\epsilon = 10$				
Algorithm Type		$D=2$	$D=16$	$D=64$	$D=128$	$D=2$	$D=16$	$D=64$	$D=128$	$D=2$	$D=16$	$D=64$	$D=128$	
Best algorithm on benchmark [†]		Varies	0.016	0.05	0.25	0.22	0.005	0.09	0.56	0.12	0.01	0.02	0.15	0.23
	DSBM [†]	0.03	0.18	0.7	2.26	0.04	0.09	1.9	7.3	0.26	102	3563	15000	
	SF ² M-Sink [†]	0.04	0.18	0.39	1.1	0.07	0.3	4.5	17.7	0.17	4.7	316	812	
	ASBM (ours)	0.016	0.1	0.85	11.05	0.02	0.34	1.57	3.8	0.013	0.25	1.7	4.7	

Table 2: Comparisons of BW_2^2 -UVP \downarrow (%) between the ground truth target distribution $p_1(x_1)$ and learned target distribution $q_\theta(x_1)$. The best metric over *bridge matching algorithms* is **bolded**. Results marked with [†] are taken from [11].

Remark. There exist recent light SB algorithms [21, 11] which do not use neural parameterization and rely on the Gaussian mixtures instead. However, these methods have very strong inductive bias towards the benchmark as it is also constructed using Gaussian mixtures. Therefore, we exclude them from comparison, see the comments of the authors in [21, §5.2] and [11, §5.2]

C.3 Colored MNIST

Here we test ASBM (ours, NFE=4) and DSBM (NFE=100) algorithms starting from mini-batch OT coupling [45] on transfer between colorized MNIST digits of classes "2" and "3" with $\epsilon \in \{1, 10\}$. We learn ASBM and DSBM on *train* set of digits and show the translated *test* images in Figures 6 and 7 along with calculated *test* FID in Table 3.

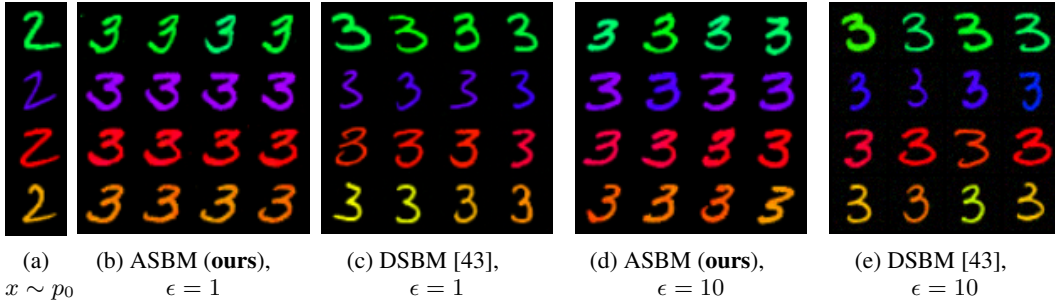


Figure 6: Samples from ASBM (ours) and DSBM learned on Colored MNIST 2 \rightarrow 3 (32×32) translation for $\epsilon \in \{1, 10\}$.

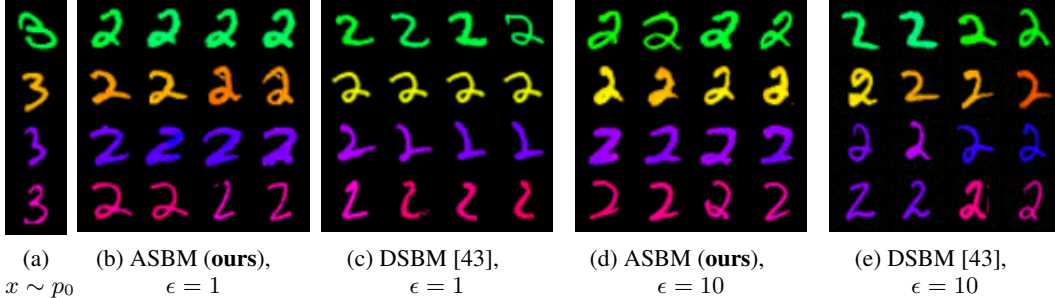


Figure 7: Samples from ASBM (ours) and DSBM learned on Colored MNIST 3 \rightarrow 2 (32×32) translation for $\epsilon \in \{1, 10\}$.

For $\epsilon = 1$ the color stays almost exactly the same through translation and there are minor shape diversity for both ASBM and DSBM, see Figures (6b, 6c, 7b, 7c). In turn, $\epsilon = 10$ introduces more stochasticity to the solutions, and expectedly the color and shape vary a bit but overall stays similar to input data for both ASBM and DSBM, see Figures (6d, 6e, 7d, 7e). As one can see from Table 3,

Model	ϵ	FID (2 \rightarrow 3)	FID (2 \rightarrow 3)
ASBM (ours)	1	2.7	2.8
DSBM	1	6.2	5.3
ASBM (ours)	10	4.3	4.53
DSBM	10	58.7	59.9

Table 3: C-MNIST FID values for ASBM and DSBM with $\epsilon \in \{1, 10\}$

ASBM has better FID on both $\epsilon \in \{1, 10\}$. However DSBM experiences a notable increase in FID with $\epsilon = 10$. We conjecture that this is due to the FID instability w.r.t. slightly noisy images which may appear in DSBM because of the necessity to integrate noisy trajectories (for large ϵ).

D Experimental Details

D.1 Details of DDGAN Implementation for Learning Markovian Projection

Below, we discuss the parametrization of the discriminator and generator in detail. In general we follow [49], but we change their DDPM diffusion inner process on the Brownian bridge process.

Parametrization and objective for the discriminator. As in the DD-GAN paper [49] we use a time-conditional discriminator $D_\xi(x_t, x_{t_{n-1}}, t_{n-1}) : \mathbb{R}^D \times \mathbb{R}^D \times [0, 1] \rightarrow [0, 1]$. For each time moment t and object $x_{t_{n-1}}$, the role of this discriminator is to check whether the sample x_t is from the distribution $q(x_t | x_{t_{n-1}})$. As well as in the DD-GAN paper [49], we train this discriminator by optimizing the following objective:

$$\min_{\xi} \sum_{n=1}^{N+1} \mathbb{E}_{q(x_{t_{n-1}})} [\mathbb{E}_{q(x_t | x_{t_{n-1}})} [-\log D_\xi(x_t, x_{t_{n-1}}, t_{n-1})] + \mathbb{E}_{q_\theta(x_t | x_{t_{n-1}})} [-\log(1 - D_\xi(x_t, x_{t_{n-1}}, t_{n-1}))]] \quad (35)$$

Here, the samples from $q(x_t | x_{t_{n-1}})$ play the role of true samples, while the samples obtained from the parametrized distribution $q_\theta(x_t | x_{t_{n-1}})$ play role of fake samples in terms of original GANs. To estimate the first expectation $\mathbb{E}_{q(x_{t_{n-1}})} \mathbb{E}_{q(x_t | x_{t_{n-1}})} = \mathbb{E}_{q(x_t, x_{t_{n-1}})}$ one should sample from $q(x_t, x_{t_{n-1}})$. To sample a pair $(x_t, x_{t_{n-1}}) \sim q(x_t, x_{t_{n-1}})$, we use the properties (5) and (6) of the reciprocal process q :

$$q(x_t, x_{t_{n-1}}) = \int p^{W^\epsilon}(x_t | x_{t_{n-1}}, x_1) p^{W^\epsilon}(x_{t_{n-1}} | x_0, x_1) q(x_1, x_0) dx_1 dx_0.$$

Sampling from $q(x_{t_{n-1}}) q_\theta(x_t | x_{t_{n-1}})$ for estimation of second expectation is given in detail below.

Parametrization and objective for the generator. We follow the same setup as the authors of DD-GAN [49] and parametrize $q_\theta(x_t | x_{t_{n-1}})$ implicitly through the generator $G_\theta(x_{t_{n-1}}, z, t) : \mathbb{R}^D \times \mathbb{R}^Z \times [0, 1] \rightarrow \mathbb{R}^D$ as follows:

$$q_\theta(x_t | x_{t_{n-1}}) \stackrel{\text{def}}{=} \int_{\mathbb{R}^D} q_\theta(x_1 | x_{t_{n-1}}) p^{W^\epsilon}(x_t | x_{t_{n-1}}, x_1) dx_1 = \int_{\mathbb{R}^Z} p^{W^\epsilon}(x_t | x_{t_{n-1}}, x_1 = G_\theta(x_{t_{n-1}}, z, t)) p_z(z) dz,$$

where $q_\theta(x_1 | x_{t_{n-1}})$ should match $q(x_1 | x_{t_{n-1}})$ and $p_z(z)$ is the auxiliary probability distribution for the generator G_θ to model samples from $q_\theta(x_1 | x_{t_{n-1}})$. Thus, for a given $x_{t_{n-1}}$ sample $x_t \sim q_\theta(x_t | x_{t_{n-1}})$ is obtained by first sampling x_1 from the generator G_θ and then using sampling from the Brownian bridge $p^{W^\epsilon}(x_t | x_{t_{n-1}}, x_1)$. While in the DD-GAN, the authors use the intermediate time distribution $q(x_{in} | x_0, x_1)$ from DDPM [15] and it is the main difference between our Markovian projection and one which the authors of DD-GAN used. As in the non-saturation GANs [10], we train the generator by optimizing the following objective:

$$\max_{\theta} \sum_{n=1}^{N+1} \mathbb{E}_{q(x_{t_{n-1}})} \mathbb{E}_{q_\theta(x_t | x_{t_{n-1}})} [\log(D_\phi(x_t, x_{t_{n-1}}, t_{n-1}))].$$

D.2 Details of D-IMF Implementation

General description of the ASBM algorithm. D-IMF algorithm is parametrized by the number K of outer D-IMF iterations, number of inner D-IMF iterations (number of generator gradient optimization steps inside one IMF iteration), ASBM number of inner steps N and starting coupling $q^0(x_0, x_1)$ used in the initial reciprocal process $q^0(x_0, x_{\text{in}}, x_1) = p^{W^\epsilon}(x_{\text{in}}|x_0, x_1)q^0(x_0, x_1)$. Our ASBM Algorithm 1 for D-IMF procedure is analog of DSBM [43, Algorithm 1] for IMF procedure.

Algorithm 1: Adversarial SB matching (ASBM).

Input : number of intermediate steps N ;
initial process $q^0(x_0, x_{t_1}, \dots, x_{t_N}, x_1)$ accessible by samples;
number of outer iteration $K \in \mathbb{N}$;
forward transitional density network $\{q_\theta(x_{t_n}|x_{t_{n-1}})\}_{n=1}^{N+1}$;
backward transitional density network $\{q_\eta(x_{t_{n-1}}|x_{t_n})\}_{n=1}^{N+1}$;

Output : $p_0(x_0) \prod_{n=1}^{N+1} q_\theta(x_{t_n}|x_{t_{n-1}}) \approx p_1(x_1) \prod_{n=1}^{N+1} q_\eta(x_{t_{n-1}}|x_{t_n}) \approx p^{T^*}(x_0, x_{\text{in}}, x_1)$.

for $k = 0$ to $K - 1$ **do**

- Learn $\{q_\theta(x_{t_n}|x_{t_{n-1}})\}_{n=1}^{N+1}$ using 15 with q^{4k} ;
- Let q^{4k+1} be given by $p_0(x_0) \prod_{n=1}^{N+1} q_\theta(x_{t_n}|x_{t_{n-1}})$;
- Let q^{4k+2} be given by $p^{W^\epsilon}(x_{\text{in}}|x_0, x_1)q_\theta(x_0, x_1)$;
- Learn $\{q_\eta(x_{t_{n-1}}|x_{t_n})\}_{n=1}^{N+1}$ using 16 with q^{4k+2} ;
- Let q^{4k+3} be given by $p_1(x_1) \prod_{n=1}^{N+1} q_\eta(x_{t_{n-1}}|x_{t_n})$;
- Let q^{4k+4} be given by $p^{W^\epsilon}(x_{\text{in}}|x_0, x_1)q_\eta(x_0, x_1)$;

We do not reinitialize neural networks during the ASBM algorithm.

Special pretraining on the 0-th outer iteration. While, in general, Algorithm 1 implements our scheme, in our experiments, we slightly modify the initial outer iteration based on purely empirical reasons. We train both forward and backward models $\{q_\theta(x_{t_n}|x_{t_{n-1}})\}_{n=1}^{N+1}$ and $\{q_\eta(x_{t_{n-1}}|x_{t_n})\}_{n=1}^{N+1}$ with q^0 and the let q^1 be $p_0(x_0) \prod_{n=1}^{N+1} q_\theta(x_{t_n}|x_{t_{n-1}})$. We use more gradient setups on this iteration than on the further outer iterations. We do that to "pretrain" both processes q_θ and q_η to model p_1 and p_0 respectively. Then we proceed to other iterations as described in Algorithm 1.

D.3 Hyperparameters of ASBM

For all the experiments, Discrete Markovian Projection is conducted using the DD-GAN code [49]:

<https://github.com/NVlabs/denoising-diffusion-gan>

The only thing that we modify is the replacement of the DDPM [15] posterior sampling for generator with our Brownian Bridge posterior sampling, see Appendix D.1.

In Toy 2D (Appendix C.1) and SB Benchmark (Appendix C.2) experiments, both generator and discriminator are parametrized by MLPs with inner layer widths [256, 256, 256], LeakyReLU activations and 2-dimensional time embeddings using `torch.nn.Embeddings`. In CelebA (§4.2) and Colored MNIST (Appendix C.3) experiments, generator is parametrized by U-Net [38] and discriminator by a ResNet-like architectures with addition of positional time encoding as in [49]. Neural networks are optimized with the Adam optimizer [19] and apply the Exponential Moving Averaging (EMA) on generator's weights. At the start of a new D-IMF iteration, both the generator, generator (EMA), discriminator and optimizers are initialized using checkpoints from the end of the previous D-IMF iteration. Inside each D-IMF iteration (except the initial one), EMA generator weights are used for sampling from previous Discrete Markovian Projections. Starting coupling $q^0(x_0, x_1)$ may be either Ind, i.e. $q^0(x_0, x_1) = p_0(x_0)p_1(x_1)$, or Mini Batch Optimal Transport coupling (MB), i.e. discrete Optimal Transport solved on mini-batch samples [45].

The hyperparameters which we use in the experiments are summarized in Table 4.

Other details & pre-processing. Test FID is calculated using `pytorch-fid` package. Working with CelebA dataset [30], we use all 84434 male and 118165 female samples (90% train, 10% test of each class). Each sample is resized to 128×128 and normalized by 0.5 mean and 0.5 std. Generator and

Experiment	Start coupling $q^0(x_0, x_1)$	D-IMF outer iters	D-IMF=0 grad updates	D-IMF grad updates	N	Batch Size	D/G opt ratio	EMA decay	Lr G	Lr D
2D Toy	Ind	20	400000	40000	3	512	1:1	0.999	1e-4	1e-4
SB Bench	Ind	2	133000	67000	31	128	3:1	0.999	1e-4	1e-4
C-MNIST	MB	3	100000	50000	3	64	1:1	0.999	1.25e-4	1.6e-4
CelebA	MB	5	1000000	40000	3	32	1:1	0.9999	1.25e-4	1.6e-4

Table 4: Hyperparameters for experiments. D stands for Discriminator and G stands for Generator. Ratio of Discriminator optimization steps w.r.t. Generator optimization steps is denoted by D/G opt ratio. Lr stands for learning rate.

discriminator are the same as for CelebA-HQ in DDGAN [49] (42M Generator parameters and 27M Discriminator parameters). Working with Colorized MNIST [12], we pick digits of classes "2" and "3" (we use the default MNIST *train/test* split), resize them to 32×32 and normalize by 0.5 mean and 0.5 std. We use the same generator and discriminator as DDGAN uses in CIFAR10 [49].

Computational time. The most time challenging experiment on CelebA runs for approximately 7 days on 1 GPU A100. Experiment with Colored MNIST takes less than 2 days of training on GPU A100. Toy2D and Schrödinger Bridge benchmark experiments take several hours on GPU A100.

D.4 Details of DSBM Baseline

DSBM [43] implementation is taken from the official code:

<https://github.com/yuyang-shi/dsbm-pytorch>

For CelebA experiment all the hyperparameters, except for 200k training iterations for the first IMF iteration (Bridge Matching **pretrain**, Appx I.3 [43]) and number of overall IMF iterations (that is taken the same as for corresponding ASBM experiment, see Table 4), were taken from [43]. As a neural network time conditional U-Net model (38M parameters) was used. Hyperparameters and neural network for Colored MNIST experiment were taken from MNIST \leftrightarrow E-MNIST experiment [43, §6]. Starting coupling is used exactly the same as for ASBM in corresponding experiments, see Table 4.

E Additional results on CelebA

E.1 Analysis on D-IMF/IMF iterations dynamics

We include additional analysis on dynamics of model samples with D-IMF iterations for ASBM (ours) and IMF iterations for DSBM with $\epsilon = 1$. As one can see from Figure 9a ASBM visually almost converges after 5 iterations in terms of similarity of generated sample w.r.t. to input data, i.e., the transport cost. From plot in Figure 8 we see that ASBM’s FID does not change through subsequent D-IMF iterations; ASBM fits target on the iteration 5 rather well. Looking at Figure 9b, one can conclude that for DSBM visual similarity along side with transport cost starts to diverge after 5th outer IMF iteration. Also, as it can be seen at plot in Figure 8, FID stops to improve after outer iteration 9 and does not improve drastically from outer iteration 5. Hence, we take ASBM and DSBM with 5 outer D-IMF/IMF iterations as a balance point for our comparison.

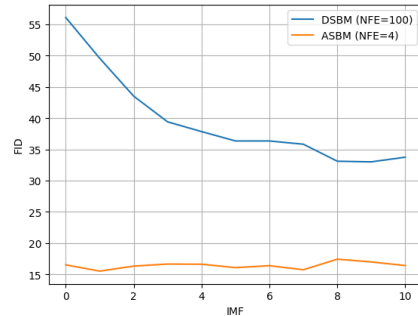
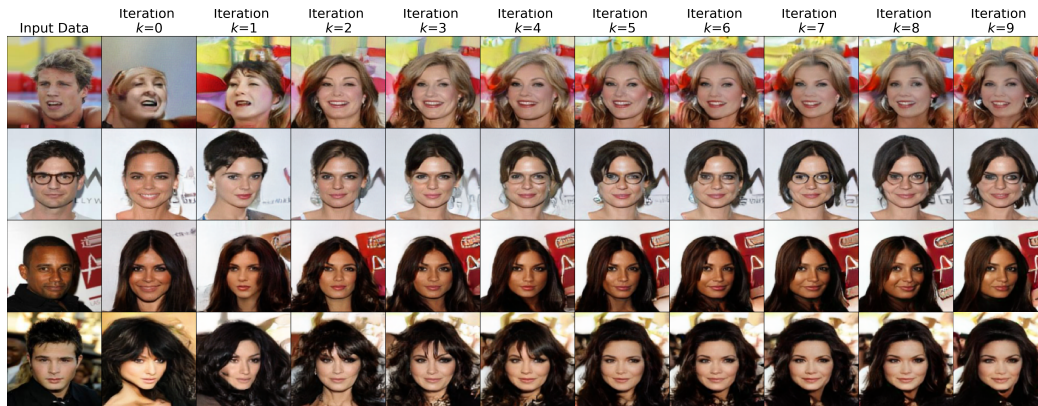


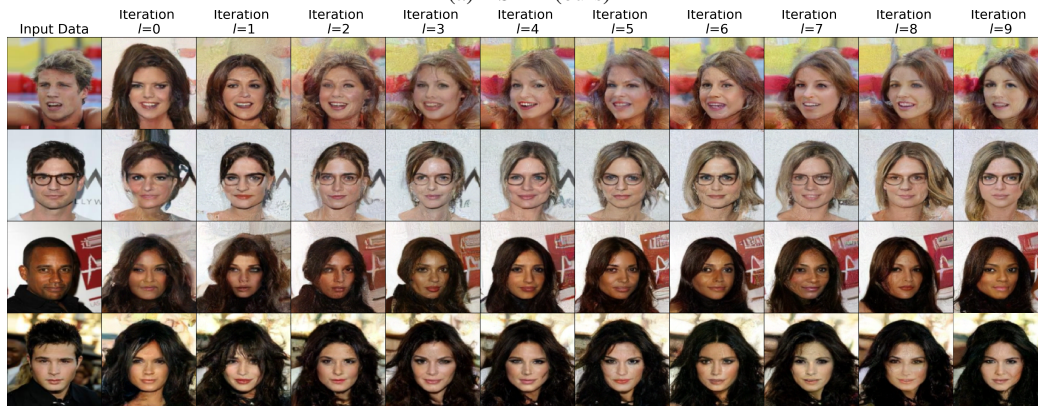
Figure 8: ASBM and DSBM FID w.r.t. IMF iterations.

E.2 ASBM (ours) and DSBM samples for *female* \rightarrow *male* (128×128)

In Figure 10, we provide additional examples for *female* \rightarrow *male* (128×128) setting with $\epsilon \in \{1, 10\}$ for ASBM (Figures 10b, 10e) and DSBM (Figures 10c, 10f) along with quantitative evaluation of FID values. Both ASBM and DSBM models were evaluated at D-IMF/IMF iteration number 4. As one can see ASBM (NFE=4) outperforms DSBM (NFE=100) in FID using only 4 evaluation steps.



(a) ASBM (ours)



(b) DSBM

Figure 9: Samples dependence on D-IMF/IMF outer iterations number k , $\epsilon = 1$.

E.3 Extra (uncurated) samples for ASBM (ours) on CelebA $male \leftrightarrow female$ (128×128)

In Figures 11 and 12, we provide additional samples for ASBM CelebA $male \leftrightarrow female$ (128×128) experiment with $\epsilon \in \{1, 10\}$.

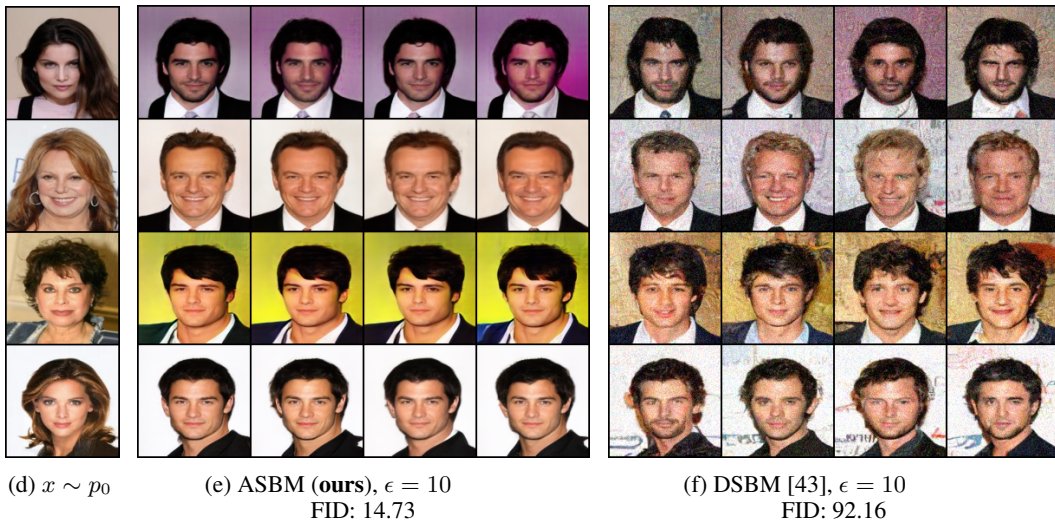
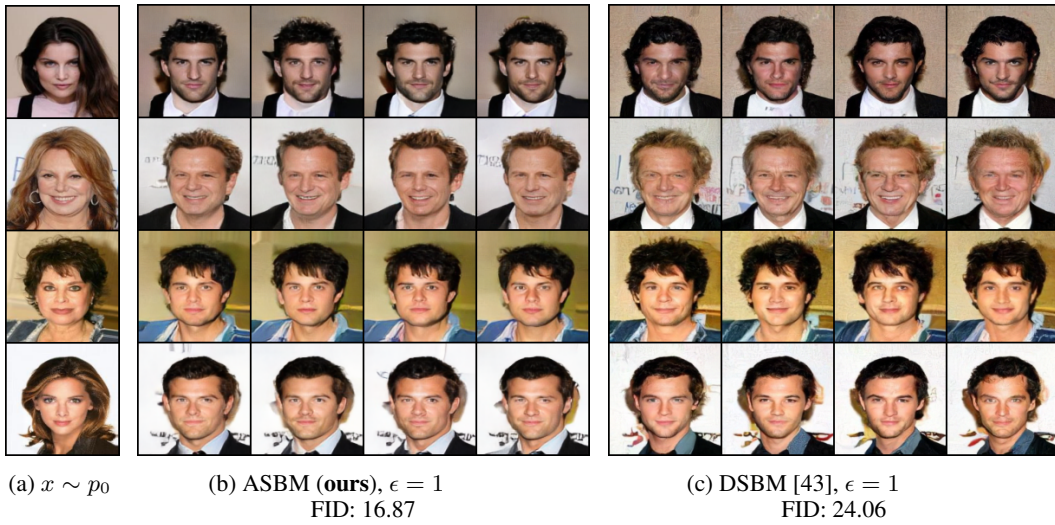
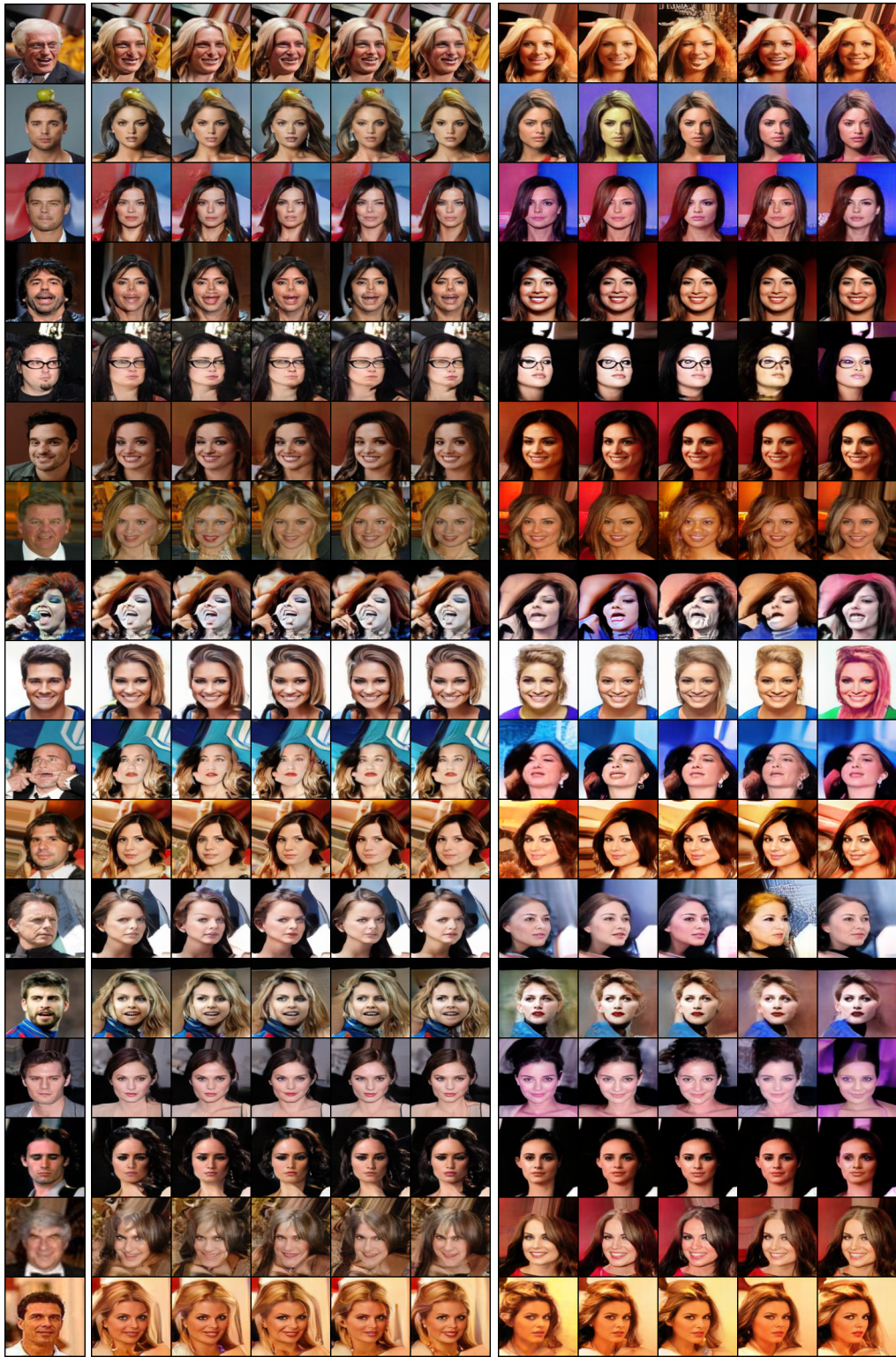


Figure 10: Samples from ASBM (ours) and DSBM learned on Celeba *female*→*male* (128×128) for $\epsilon \in \{1, 10\}$



(a) Input

(b) Output for $\epsilon = 10$

(c) Output for $\epsilon = 10$

Figure 11: ASBM (ours) Celeba *male*→*female* (128×128) samples for $\epsilon \in \{1, 10\}$



(a) Input

(b) $\epsilon = 10$

(c) $\epsilon = 10$

Figure 12: ASBM *female*→*male* (128×128) samples for $\epsilon \in \{1, 10\}$